



**HAL**  
open science

## Neuroprotective Effect of Maternal Resveratrol Supplementation in a Rat Model of Neonatal Hypoxia-Ischemia

Ursule Dumont, Stéphane Sanchez, Cendrine Repond, Marie-Christine  
Beauvieux, Jean-François Chateil, Luc Pellerin, Anne-Karine Bouzier-Sore,  
Hélène Roumes

► **To cite this version:**

Ursule Dumont, Stéphane Sanchez, Cendrine Repond, Marie-Christine Beauvieux, Jean-François Chateil, et al.. Neuroprotective Effect of Maternal Resveratrol Supplementation in a Rat Model of Neonatal Hypoxia-Ischemia. *Frontiers in Neuroscience*, 2021, 14, 10.3389/fnins.2020.616824 . hal-03376677

**HAL Id: hal-03376677**

**<https://hal.science/hal-03376677v1>**

Submitted on 15 Oct 2021

**HAL** is a multi-disciplinary open access archive for the deposit and dissemination of scientific research documents, whether they are published or not. The documents may come from teaching and research institutions in France or abroad, or from public or private research centers.

L'archive ouverte pluridisciplinaire **HAL**, est destinée au dépôt et à la diffusion de documents scientifiques de niveau recherche, publiés ou non, émanant des établissements d'enseignement et de recherche français ou étrangers, des laboratoires publics ou privés.

# Neuroprotective effect of maternal resveratrol supplementation in a rat model of neonatal hypoxia-ischemia

Ursule Dumont<sup>1,2</sup>, Stéphane Sanchez<sup>1</sup>, Cendrine Repond<sup>2</sup>, Marie-Christine Beauvieux<sup>1</sup>, Jean-François Chateil<sup>1</sup>, Luc Pellerin<sup>2,3</sup>, Anne-Karine Bouzier-Sore<sup>1</sup>, Hélène Roumes<sup>1\*</sup>

<sup>1</sup>UMR5536 Centre de Résonance Magnétique des Systèmes Biologiques (CRMSB), France, <sup>2</sup>Department of Physiology, University of Lausanne, Switzerland, <sup>3</sup>INSERM U1082 Ischémie Reperfusion en Transplantation d'Organes Mécanismes et Innovations Thérapeutiques, France

*Submitted to Journal:*  
Frontiers in Neuroscience

*Specialty Section:*  
Neuroenergetics, Nutrition and Brain Health

*Article type:*  
Original Research Article

*Manuscript ID:*  
616824

*Received on:*  
13 Oct 2020

*Frontiers website link:*  
[www.frontiersin.org](http://www.frontiersin.org)

In review

### *Conflict of interest statement*

The authors declare that the research was conducted in the absence of any commercial or financial relationships that could be construed as a potential conflict of interest

### *Author contribution statement*

UD has acquired and analyzed data, and has contributed to the final drafting of the article. SS has produced the HI neonate model. CR has participated to Western-Blot and RTqPCR experiments. MCB and JFC have contributed to the final drafting of the article. LP have contributed to the design of the experiments and wrote the article. AKBS and HR have conceived, designed, acquired and analyzed data, and wrote the article.

### *Keywords*

polyphenol, resveratrol, Neonatal hypoxia-ischemia, brain metabolism, MRI

### *Abstract*

Word count: 341

Neonatal hypoxia-ischemia (HI) is a major cause of death or subsequent disabilities in infants. HI causes brain lesions, which are induced by a strong reduction in oxygen and nutrient supply. Hypothermia is the only validated beneficial intervention, but not all newborns respond to it and today no pharmacological treatment exists. Among possible therapeutic agents to test, trans-resveratrol (RSV) is an interesting candidate as it has been reported to exhibit neuroprotective effects in some neurodegenerative diseases. This experimental study aimed to investigate a possible neuroprotection of RSV in rat neonatal HI, when administered to the pregnant rat female, at a nutritional dose. Several groups of pregnant female rats were studied in which RSV was added to drinking water either during the last week of pregnancy, the first week of lactation, or both. Then, 7-day old pups underwent an HI event. Pups were followed longitudinally, using both MRI and behavioral testing. Finally, a last group was studied in which breast-feeding females were supplemented one week with RSV just after the HI event of the pups (to test the curative rather than the preventive effect). To decipher the molecular mechanism of this neuroprotection, RT-qPCR and western blots were also performed on pup brain samples. Data clearly indicated that when dams were supplemented with RSV, HI pup brain lesions were significantly reduced. Moreover, inside the lesion, the severity of edema was considerably improved by RSV in the striatum and the hippocampus. Maternal RSV supplementation allowed to reverse HI pup sensorimotor and cognitive deficits caused by the insult. The best recoveries were observed when RSV was administered during both gestation and lactation (2 weeks before the HI event in pups). Furthermore, RSV neuroprotection was also observed in the curative group, but only at the latest stages examined. Our hypothesis is that RSV, in addition to the well-known neuroprotective benefits via the sirtuin's pathway (antioxidant properties, inhibition of apoptosis), has an impact on brain metabolism, and more specifically on the astrocyte-neuron lactate shuttle (ANLS), as suggested by RT-qPCR and western-blot data that contributes to the neuroprotective effects.

### *Contribution to the field*

Dear Editor, Our manuscript entitled: « Neuroprotective effect of maternal resveratrol supplementation in a rat model of neonatal hypoxia-ischemia » by Dumont et al. has been submitted to your journal, Frontiers in Cellular Neuroscience, in the special issue "Polyphenols' Action on the Brain". In this study, we present a new therapeutic approach to counteract neonatal hypoxia-ischemia brain damages. The originality of our work is dual. First, we used Resveratrol, a polyphenol that is thought to be neuroprotective. Second, a transgenerational and nutritional approach was applied. Indeed, in our study, only the pregnant and breastfeeding female was supplemented with Resveratrol, to a much lower dose compared to what can be found in the literature. The impact of this supplementation was followed by MRI and we took advantage of this non-invasive technique to perform a longitudinal study coupled to behavioral tests. Neuroprotection on brain lesions on the pups that underwent hypoxia-ischemia was clearly demonstrated. Moreover, we performed gene and protein expression analysis to decipher the mechanism of this neuroprotection. In addition to the "classical" anti-oxidant and anti-apoptotic pathways, we demonstrated, for the first time, the role of resveratrol on brain metabolism modulation. We think that our results can be further transferred to the clinic. We believe that this study is perfectly within the scope of your journal and this special issue and that it will be of great interest for your readers. In the hope of receiving rapidly a positive answer from your journal, Sincerely yours, Dr H el ene Roumes PS: Please, note that this is my inaugural article, as I've been recently nominated as an Associate Editor in Frontiers.

### *Funding statement*

This work was supported by grants (2018/01) from the Fondation de Recherche en Alcoologie (FRA), from the French State in the context of the "Investments for the future" Programme IdEx (ANR-10-IDEX), the LabEx TRAIL(Translational Research and Advanced Imaging Laboratory) cluster of excellence of Bordeaux University (ANR-10-LABX-57) and the Department of Physiology, University of Lausanne. LP received financial support from the program IdEx Bordeaux ANR-10-IDEX-03-02.

### *Ethics statements*

#### *Studies involving animal subjects*

Generated Statement: The animal study was reviewed and approved by Bordeaux ethic committee.

#### *Studies involving human subjects*

Generated Statement: No human studies are presented in this manuscript.

#### *Inclusion of identifiable human data*

Generated Statement: No potentially identifiable human images or data is presented in this study.

#### *Data availability statement*

Generated Statement: The datasets presented in this study can be found in online repositories. The names of the repository/repositories and accession number(s) can be found in the article/supplementary material.

In review

1 **Neuroprotective effect of maternal resveratrol supplementation in a rat**  
2 **model of neonatal hypoxia-ischemia**

3 **Ursule Dumont<sup>1</sup>, Stéphane Sanchez<sup>1</sup>, Cendrine Repond<sup>2</sup>, Marie-Christine Beauvieux<sup>3</sup>, Jean-**  
4 **François Chateil<sup>3</sup>, Luc Pellerin<sup>1,4,#</sup>, Anne-Karine Bouzier-Sore<sup>1,#</sup> and Hélène Roumes<sup>1,#,\*</sup>**

5 <sup>1</sup>Univ. Bordeaux, CNRS, CRMSB, UMR 5536, F-33076 Bordeaux, France

6 <sup>2</sup>Département de Physiologie, University of Lausanne, Switzerland

7 <sup>3</sup>CHU de Bordeaux, Place Amélie Raba Léon 33000 Bordeaux

8 <sup>4</sup>Inserm U1082, Université de Poitiers, 86021 Poitiers

9 # : Same contribution

10

11 **Correspondence:**

12 \*: Corresponding Author

13 Hélène Roumes: [helene.roumes@rmsb.u-bordeaux.fr](mailto:helene.roumes@rmsb.u-bordeaux.fr)

14

15 **Keywords: Polyphenol, resveratrol, neonatal hypoxia-ischemia, brain metabolism, MRI**

16

17 **Abstract**

18 Neonatal hypoxia-ischemia (HI) is a major cause of death or subsequent disabilities in infants. HI  
19 causes brain lesions, which are induced by a strong reduction in oxygen and nutrient supply.  
20 Hypothermia is the only validated beneficial intervention, but not all newborns respond to it and today  
21 no pharmacological treatment exists. Among possible therapeutic agents to test, trans-resveratrol  
22 (RSV) is an interesting candidate as it has been reported to exhibit neuroprotective effects in some  
23 neurodegenerative diseases. This experimental study aimed to investigate a possible neuroprotection  
24 of RSV in rat neonatal HI, when administered to the pregnant rat female, at a nutritional dose. Several  
25 groups of pregnant female rats were studied in which RSV was added to drinking water either during  
26 the last week of pregnancy, the first week of lactation, or both. Then, 7-day old pups underwent an HI  
27 event. Pups were followed longitudinally, using both MRI and behavioral testing. Finally, a last group  
28 was studied in which breast-feeding females were supplemented one week with RSV just after the HI  
29 event of the pups (to test the curative rather than the preventive effect). To decipher the molecular  
30 mechanism of this neuroprotection, RT-qPCR and western blots were also performed on pup brain  
31 samples. Data clearly indicated that when dams were supplemented with RSV, HI pup brain lesions  
32 were significantly reduced. Moreover, inside the lesion, the severity of edema was considerably  
33 improved by RSV in the striatum and the hippocampus. Maternal RSV supplementation allowed to  
34 reverse HI pup sensorimotor and cognitive deficits caused by the insult. The best recoveries were

35 observed when RSV was administered during both gestation and lactation (2 weeks before the HI event  
36 in pups). Furthermore, RSV neuroprotection was also observed in the curative group, but only at the  
37 latest stages examined. Our hypothesis is that RSV, in addition to the well-known neuroprotective  
38 benefits *via* the sirtuin's pathway (antioxidant properties, inhibition of apoptosis), has an impact on  
39 brain metabolism, and more specifically on the astrocyte-neuron lactate shuttle (ANLS), as suggested  
40 by RT-qPCR and western-blot data that contributes to the neuroprotective effects.

41

## 42 **1 Introduction**

43 Neonatal hypoxic-ischemic encephalopathy (HIE) is the most common cause of perinatal brain injury,  
44 which may lead to neonatal death or irreversible damages like permanent physical disabilities, cerebral  
45 palsy and cognitive dysfunctions (Shankaran, 2012). HIE has a high global incidence of 1-8 per 1,000  
46 live births, and remains a major cause of infantile mortality (Kurinczuk et al., 2010). It is caused by a  
47 massive reduction in cerebral blood flow and, therefore, oxygen and glucose supply to the brain. Today,  
48 the only applied treatment is moderate hypothermia (Gluckman et al., 2005), which cools down  
49 newborns to 33-34°C and is used in a time-window of 72 h after the hypoxic-ischemic event (Bona et  
50 al., 1998). However, this treatment is only partly efficient and is unsuccessful for nearly half of the  
51 patients (Wu and Gonzalez, 2015). Therefore, there is an urgent need to find a complementary therapy  
52 to further reduce the rate and severity of neurodevelopmental disabilities resulting from HIE.

53 According to the literature, evidence exists about the neuroprotective properties of *trans*-resveratrol  
54 (RSV) in the context of neonatal HIE (West et al., 2007). RSV (3,5,4'-trihydroxystilbene) is a natural  
55 polyphenol present at relatively high concentrations in peanuts, grape skin and seeds. RSV possess  
56 interesting biological properties such as anti-inflammatory (Das and Das, 2007), anti-oxidant (Gao et  
57 al., 2018) and anti-apoptotic activities (Bian et al., 2017). These activities may have promising potential  
58 therapeutic applications, as shown *in vivo* (Baur and Sinclair, 2006). Increasing evidence indicates that  
59 RSV may also play a role in the prevention of neurodegenerative diseases, such as Alzheimer's disease  
60 or Parkinson's disease (Sawda et al., 2017). Interestingly, blood-borne RSV can cross the blood-brain  
61 barrier (BBB) (Baur and Sinclair, 2006).

62 During the last decade, this polyphenol has shown a neuroprotective effect both as a *pre*- and *post*-  
63 treatment in the context of neonatal hypoxia-ischemia (HI) (West et al., 2007; Karalis et al., 2011;  
64 Arteaga et al., 2015; Pan et al., 2016; Bian et al., 2017; Gao et al., 2018). Indeed, when administered  
65 just after the HI event (intraperitoneal injection (i.p.); 90mg/kg), data indicated that RSV is  
66 neuroprotective as demonstrated by a strong reduction of the infarct volume and by the recovery of  
67 some behavioral functions (Karalis et al., 2011). This neuroprotection was also observed when RSV  
68 was administered before the HI event (Arteaga et al., 2015). When RSV was injected 10 minutes before  
69 the HI event (i.p.; 20 mg/kg; using the classical Rice-Vannucci P7 pup model), a reduction in lesion  
70 volumes and an improvement of cognitive and motor functions (long-term assessment) were observed  
71 (Arteaga et al., 2015). The administration of RSV before the HI episode seems even more  
72 neuroprotective than when administered after.

73 Taking into account the fact that (i) maternal supplementation has an impact not only on pregnant  
74 women but also on the fetus (Nnam, 2015), (ii) RSV has neuroprotective properties and (iii) RSV and  
75 its metabolites can cross the placental and the BBB barriers (Bourque et al., 2012; Shankaran, 2012),  
76 we aimed to evaluate the neuroprotective role of maternal RSV supplementation, at nutritional dose,  
77 in a context of neonatal HI. The originality of our approach combines (i) a transgenerational and

78 nutritional approach, (ii) a longitudinal study of brain lesion evolution using non-invasive MRI  
79 associated to several behavioral tests, and (iii) a study of some gene and protein expressions in the  
80 brain of pups to try to decipher the molecular mechanisms of this neuroprotection. For this purpose,  
81 expression of sirtuins (SIRT1), superoxide dismutase (SOD) and antiapoptotic proteins (Bcl2) was  
82 measured in brain samples, as well as of different key partners in brain metabolism. More particularly  
83 genes and proteins linked to the astrocyte-neuron lactate shuttle (ANLS; (Pellerin and Magistretti,  
84 1994) such as astrocytic glutamate transporters (GLT-1 and GLAST), monocarboxylate transporters  
85 (MCT1 and MCT2), lactate dehydrogenase isoforms (LDHa and LDHb) and the glial Na<sup>+</sup>/K<sup>+</sup>ATPase  
86  $\alpha_2$  isoform.

87

## 88 2 Materials and Methods

### 89 Drug administration

90 All animal procedures were conducted in accordance with the Animal Experimentation Guidelines of  
91 the European Communities Council Directive of November 24, 1986 (86/609/EEC). Protocols met the  
92 ethical guidelines of the French Ministry of Agriculture and Forests and were approved by the local  
93 ethics committee (9476). RSV was purchased from Sigma (Sigma-Aldrich, France). RSV stock  
94 solution was prepared by dissolving 100 mg of RSV in 2 ml of absolute ethanol (Sigma-Aldrich,  
95 France). A pregnant Wistar rat female drinks on average 50 ml water/day. For RSV supplementation,  
96 4  $\mu$ l of the RSV stock solution were added in 200 ml of drinking water, which results in a nutritional  
97 maternal consumption of 0.15 mg/kg/day. RSV solutions in drinking bottles were prepared and  
98 changed every day. Because of RSV photosensitivity, drinking bottles were enwrapped in aluminum  
99 foil to avoid oxidation. Four  $\mu$ l of absolute ethanol were added in drinking water (200 ml) for all sham  
100 groups during two weeks (last week of gestation + first week of breastfeeding).

101

### 102 Experimental groups

103 Pregnant Wistar female rats (Janvier Laboratories, France) were obtained at day 15 of gestation and  
104 kept on a 12h/12h light/dark cycle with A03 food (SAFE, Augy, France) and water *ad libitum*. Seven  
105 experimental groups were established according to the maternal supplementation plan (Figure 1).

106 Three control groups were first considered. The **sham** group for which there was no maternal RSV  
107 supplementation and in which pups did not undergo a HI episode but only carotid exposition (n=18).  
108 The **shamrsv group**, for which RSV was added to the dam's drinking water during the last week of  
109 gestation and the first week of lactation and in which pups did not undergo a HI episode (only carotid  
110 exposition). This control group was performed to ensure that RSV had no effect on healthy pups (see  
111 supplementary Figure 1, n=6). Finally, the **HIC** group, without maternal RSV supplementation and in  
112 which pups underwent an HI event at P7 (n=31). One preliminary study was performed on this **HIC**  
113 group to ensure the reproducibility of the model (n=11).

114 In a second step, four supplementation groups in which pups underwent an HI event at postnatal day 7  
115 (P7) were considered: pups from a pregnant female that received RSV supplementation in drinking  
116 water (i) both during the first week of lactation and the last week of gestation (gestation + lactation  
117 group; **rsvGL** group; n=15), (ii) only the last week of gestation (gestation group; **rsvG** group; n=15),

118 (iii) only the first week of lactation (lactation group; **rsvL**; n=15), or (iv) only the second week of  
119 lactation (one week after the HI event; curative group; **rsvC** group; n=15).

120

## 121 **Model of neonatal hypoxic-ischemic brain injury**

122 Cerebral HI was performed using the Rice and Vannucci model (Rice et al., 1981) as described  
123 previously (Dumont et al., 2019). Briefly, postnatal day 7 (P7) rat pups of both genders were used in  
124 the experiment (due to no statistical difference between males and females in our study, data from both  
125 genders were pooled). Pups weighing 15-19 g were anesthetized using isoflurane (4 % for induction  
126 and 1.5 % for maintenance). For ischemia, neck skin and muscles along an anterior midline were  
127 incised and the left common carotid artery was permanently ligated (surgery duration never exceeded  
128 10 min per pup). After surgery, pups were placed in a heated atmosphere ( $33 \pm 1^\circ\text{C}$ ) during 30 min in  
129 order to recover. Hypoxia was induced by placing animals during 2 h in a hypoxic chamber (Intensive  
130 Care Unit Warmer, Harvard Apparatus, Les Ulis, France, 8 %  $\text{O}_2$ , 92 %  $\text{N}_2$ ). The hypoxic chamber  
131 temperature was maintained at  $33 \pm 1^\circ\text{C}$  to ensure a pup rectal temperature of  $35.5 \pm 0.5^\circ\text{C}$   
132 (normothermia) and 80% humidity. For sham pups (sham and shamrsv groups), the left common  
133 carotid artery was just exposed (under the same anesthetic procedure as described above) and after 30  
134 min of recovery, pups were kept separated from the dam in a heated atmosphere ( $33 \pm 1^\circ\text{C}$ , 2 h).

135

## 136 **Longitudinal frame acquisition of *in vivo* MRI**

137 MRI acquisitions were performed 2 h  $\frac{1}{2}$  after the carotid artery ligation (P7), then after 48 h (P9) and  
138 23 days later (P30), on a horizontal 4.7T Biospec 47/50 system (Bruker, Ettlingen, Germany) equipped  
139 with a 6 cm BG6 gradient system (1000 mT/m,  $\Delta = 20$  ms,  $\delta = 4$  ms). Pups were anesthetized with  
140 isoflurane (4% for induction and 1.5 % for maintenance). Breathing was monitored by a ventral  
141 pressure sensor and body temperature was maintained at  $35.5 \pm 0.5^\circ\text{C}$  during acquisition with a water-  
142 heated MRI bed. Anatomical T2-weighted images of the brain were obtained using a Rapid Acquisition  
143 with Relaxation Enhancement (RARE) sequence with 20 axial slices 0.7 mm thick, echo time (TE) =  
144 50 ms, repetition time (TR) = 3000 ms and a total duration of 4 min 48 s. Brain lesion volumes were  
145 assessed by Diffusion Weighted Imaging (DWI: 20 axial slices of 7 mm, 30 directions, b-value 1000  
146  $\text{s}/\text{mm}^2$ , TE = 24 ms, TR = 2 s,  $\Delta = 8.11$  ms,  $\delta = 2.5$  ms, total duration = 17 min 04 s). At P7, DWI was  
147 systematically performed 3 h after carotid ligation. MR-angiography was performed to image the  
148 cerebral arterial blood flow using a Time-of-Flight (TOF)-3D-Fast low angle shot (FLASH) sequence  
149 (axial slice, 20 mm thick, TE 2.2 ms, TR 13 ms, flip angle  $15^\circ$ , total duration = 10 min 59 s).  
150 Angiography was used to validate the common carotid artery ligation and the reproducibility of our  
151 neonatal HI model. Moreover, during the study, angiography was systematically performed for pups  
152 presenting no lesion at P7 to ensure that the ligation was present (see supplementary Figure 2). In two  
153 cases, pups presented no ligation and were excluded from the study.

154

## 155 **MRI analysis**

156 Measurements were performed with Paravision 6.0.1 (Bruker BioSpin, Karlsruhe, Germany). Lesion  
157 volumes were measured at P7, P9 and P30, on the diffusion-weighted images. For each rat, for each  
158 slice and on the 20 adjacent slices per rat, two region-of-interests (ROI) were manually delineated to

159 encompass the global brain area and injured area, respectively. Volume was obtained considering the  
 160 slice thickness (0.7 mm). Lesion volumes were expressed in percentage of the total brain volume.  
 161 Cytotoxic edema severity was evaluated by apparent diffusion coefficient (ADC, mm<sup>2</sup>/s) values at P7  
 162 calculated from the DWI sequences. ROIs were manually drawn such as delineating the brain lesion  
 163 inside the cortex and hippocampus in the same slice, and the striatum in another appropriate slice.

164

## 165 **Behavioral tests**

166 Behavioral tests were performed on pups from P8 to P45 (Figure 2).

### 167 ***Righting reflex (P8, P10 and P12)***

168 Righting reflex was conducted on animals from HIC, rsvGL, rsvG and rsvL groups (only groups that  
 169 had completed their supplementation window: rsvGL, rsvG and rsvL). Pups were turned on their back.  
 170 The time required to turn over on all four paws was measured. Each pup was given three attempts and  
 171 the meantime of the 3 trials was calculated.

### 172 ***Modified neurological severity score (mNSS) (P24)***

173 The mNSS test is a neurological scale widely used in the study of stroke in various models (Morris et  
 174 al., 2010). The assessment of neurological disorders is based on a scale ranging from 0 to 18. This  
 175 exam is composed of a series of motor (muscle condition, abnormal movement), sensory (visual, tactile  
 176 or proprioceptive), reflex and balance tests (18 tests). One point is awarded if the animal fails to  
 177 perform the task while no point is given if successful. Each rat was graded on the mNSS scale: the  
 178 higher the score, the more impaired the sensorimotor functions (0-1: no impairment; 2-6: moderate  
 179 impairments; 7-12: impairments; 13-18: severe impairments).

### 180 ***Novel object recognition test (P42, P43, P44 and P45)***

181 The novel object recognition test is based on the natural tendency of rodents to explore novelty  
 182 (Ennaceur and Delacour, 1988). Long-term memory was assessed in our task (Roumes et al., 2020).  
 183 After a 10-min habituation period in the open field on day 1 (P42), pups were further allowed to freely  
 184 explore two identical objects placed in opposite corners of the arena for 10 min on the next two days.  
 185 On the last day (P45), one of the old objects was replaced by a new and different one, then pups were  
 186 allowed to freely explore objects for 10 min. Durations of each object exploration were measured. The  
 187 discrimination index (score between -1 and +1) was defined as the parameter for long-term memory  
 188 evaluation:

$$189 \quad I = \left( \frac{\text{time spent on new object} - \text{time spent on familiar object}}{\text{time spent on new object} + \text{time spent on familiar object}} \right)$$

190 A positive score indicates more time spent with the new object. Closer to +1 the score is, lesser is  
 191 memory alteration.

192

## 193 **Brain sample processing**

194 Brains were collected at P9 from some pups in the supplementation group with the strongest  
195 neuroprotective effects (rsvGL group), as well as from some pups in the control and sham groups for  
196 further RT-qPCR, western blots and histology.

### 197 ***RNA and protein extractions***

198 P9 pups were lethally anesthetized with an intraperitoneal injection of Ketamine (100 mg/kg of  
199 Imalgene, Merial Boehring, Centravet Lapalisse) and Xylazine (20 mg/kg of Paxman, Virbac France,  
200 Centravet Lapalisse) then quickly decapitated. Brains were rapidly removed and placed on ice under  
201 RNase free conditions. Each structure (cortex, hippocampus and striatum) of both damaged (when  
202 possible) and undamaged sides was quickly dissected. For RT-qPCR, each brain structure sample was  
203 stored in RNAlater and for western blots it was stored in RIPA solution (Tampon Pierce™ RIPA lysis  
204 buffer 1X + inhibitor proteases cocktail 10X, Thermofisher). Then, all samples were stored at -80°C.  
205 For the most injured brains (mainly in the HIC group), the tissue loss caused by HI did not allow to  
206 collect all structures from the injured side especially the hippocampus; data for hippocampus and  
207 striatum in supplementary Figures 3 and 4).

### 208 ***Brain removal for Nissl staining***

209 P9 pups were deeply anesthetized with isoflurane. Intra-cardiac perfusion with PBS 1X was performed  
210 during 10 min (18 ml/min), followed by perfusion of a paraformaldehyde solution (PFA 4 %, in PBS  
211 1X) during 10 min (18 ml/min). Then, brains were quickly sampled and post-fixed in PFA 4 %  
212 overnight (4 °C), followed by cryoprotection in PBS 1X – Sucrose 20 % (24 hours, 4 °C) and PBS 1X-  
213 Sucrose 30% (24 hours, 4 °C). Brains were frozen with nitrogen vapor and kept at -80 °C until they  
214 were cut into 16-µm sections with a cryostat.

215

### 216 **Real-time quantitative polymerase chain reaction analysis (RT-qPCR)**

217 Total RNA was extracted and purified from each brain structure using RNeasy Protect Mini Kit  
218 (#74106, Qiagen, Hombrechtikon, Switzerland). For cDNA synthesis, 200 ng of total RNA were  
219 reverse transcribed using the Multiscribe Reverse protocol: 50 µM Random Hexamers and RT Buffer  
220 10X were added to 200 ng of samples. Samples were incubated in a thermocycler (Biometra ®,  
221 Thermocycler) 10 min at 65°C. Then, 10 mM of dNTP, MgCl<sub>2</sub>, RNase inhibitor and Multiscribe  
222 Reverse were added to the mix reaction and incubated in a thermocycler 10 min at 25°C, 45 min at  
223 48°C and 5 min at 95°C. Then, 1 µl of synthesized cDNA was subjected to RT-qPCR using the suitable  
224 primers (reverse and forward: 0.3 µM; Table 1) and SYBR Green PCR Master Mix (Applied  
225 Biosystems, Luzern, Switzerland) to perform the PCR reaction in a total reaction volume of 10 µl. Each  
226 sample was tested in triplicates. The RT-qPCR protocol was as follows: 2 ng of cDNA samples were  
227 incubated at 95°C for 3 min then 40 cycles of 3 s at 95°C and 20 s at 60°C. mRNA expression levels  
228 were determined with the StepOnePlus™ Real-Time PCR System (Applied Biosystems, Luzern,  
229 Switzerland) with RPS29 (Ribosomal Protein S29, Microsynth, Balgach, Switzerland) mRNA used as  
230 endogenous control. For data analysis, differences were calculated using the  $\Delta\Delta C_t$  method using the  
231 RPS29 gene as housekeeping gene.

232

### 233 **Western Blotting**

234 After ending experiments, brain tissues and cell lysates were prepared and protein concentrations  
235 determined with a Micro BCA Protein Assay Kit (ThermoScientific Pierce BCA Protein Assay),  
236 according to the manufacturer's recommendations. Protein concentration was adjusted in order to  
237 obtain the same concentration for each sample, and they were mixed with Laemmli Buffer 4X. Samples  
238 and molecular standards (PageRuler Prestained Protein Ladder, ThermoFisher) were loaded on a SDS-  
239 PAGE 10% polyacrylamide gel electrophoresis (PAGE), and then proteins were transferred onto a  
240 nitrocellulose membrane. Transfer (gel to membrane) was performed by semi-dry transfer (Trans Blot  
241 Turbo transfer System Bio Rad). At the end of the transfer, membranes were blocked for 1h, under  
242 agitation, at RT with TBS-T 1X (TBT- 0,1% Triton x-100), 10% Milk and 1% BSA. Then, membranes  
243 were incubated for 12h at 4°C under agitation with the appropriate primary antibody described in Table  
244 2 (MCT1 MCT2, LDHa and LDHb, 1:1000 and GLAST, 1:500). Memcode Reversible Protein Stain  
245 (Pierce) served as loading control. Blots were revealed by chemiluminescence (WesternBright ECL;  
246 Witec ag, Luzern, Switzerland) and imaged with a detection system (Chemidoc XRS+, Biorad,  
247 Switzerland). Densitometric analysis of chemiluminescent signals was performed using Image lab  
248 software.

249

### 250 **Nissl staining**

251 The 16- $\mu$ m thick brain sections were stained with cresyl violet (0.5%, Sigma-Aldrich, France) for 10  
252 min and washed in distilled water for 10 s. Sections were dehydrated in 95 and 100% ethanol (2 min  
253 each), defatted in xylene and mounted on coverslips in Depex mounting solution (Sigma Aldrich,  
254 Germany). Brain sections were observed using an optical microscope (Leica STP6000). Image J  
255 software (National institutes of Health, Bethesda, USA, <http://www.imagej.nih.gov/ij> v1.44 p)  
256 was used to count nuclei.

257

### 258 **Statistical analysis**

259 MRI quantifications were blindly performed by two separate experimenters (intra-experimenter  
260 variability < 1%; inter-experimenter variability < 5%). Statistical analysis and graphs were performed  
261 using GraphPad Prism 7.00 software. All data were expressed as mean  $\pm$  standard error of the mean  
262 (s.e.m). Number of pups is stated for each experiment within figure legends. Statistical significance of  
263 the differences between multiple groups was determined using One-Way ANOVA and Fischer's LSD  
264 post-hoc test. Statistical significance was defined as  $p < 0.05$  (\* $p < 0,05$ , \*\* $p < 0,01$ , \*\*\* $p < 0,001$  and  
265 \*\*\*\* $p < 0,0001$ ).

266

## 267 **3 Results**

### 268 ***Brain damages in the neonatal HI model***

269 All P7 pups which underwent an HI event without treatment (Rice-Vannucci model; HIC group) had  
270 a brain lesion (Figure 3A, first pie chart). Lesion volume (see typical DW image in Figure 3B, top left)  
271 represented  $42 \pm 2$  % of the total brain volume (Figure 3 C), which reflects typical lesion size after an  
272 acute HI event in this model (Ashwal et al., 2007). Forty-eight hours after HI, a 50% decrease in brain  
273 lesion volume was observed (lesion volume decreases from  $42 \pm 2$  % to  $20 \pm 2$  %, for pups in the HIC

274 group; Figure 3C). The stage reached at P9 seems to predict the final lesion size since no further  
275 evolution was measured at P30 (no statistical difference between P9 and P30) (Figure 3C and D). In  
276 addition, HI induced a drop in apparent diffusion coefficient (ADC) values in each structure (- 40%)  
277 (Figure 3E). Such a drop reflects water diffusion restriction due to cell swelling, a phenomenon typical  
278 of this time window (latent period).

### 279 ***Maternal RSV supplementation improved HI-induced brain damages***

280 Common carotid artery ligation was confirmed by angiography in all cases. Like in the control group  
281 (HIC), all pups from the gestation (rsvG) and curative (rsvC) groups exhibited brain lesions 3 h after  
282 common carotid artery ligation (P7) (Figure 3A; 3<sup>rd</sup> and 5<sup>th</sup> pie charts). When RSV was administered  
283 to the mother either during the gestation (last wk) + lactation period (1<sup>st</sup> week) (rsvGL) or during the  
284 1st week of lactation (rsvL), 20% and 13% of the pups had no brain lesion, respectively (Figure 3A;  
285 2<sup>nd</sup> and 4<sup>th</sup> pie charts). Only MRI data from P7 pups with brain damages are therefore presented for all  
286 groups.

287 Representative DW images of P7 and P30 pup brains from all groups are presented in Figure 3B. Brain  
288 lesions appear as a hyposignal at P7 (edema) whereas they appear as a hypersignal at P30 (necrotic  
289 zone). Brain lesion volumes (expressed as %, normalized to total brain volume) were calculated for  
290 different time points and values are presented in Figure 3C. At P7, no significant difference was found  
291 between pups from the HIC, rsvG and rsvC groups ( $42 \pm 2\%$ ,  $42 \pm 1\%$  and  $41 \pm 3\%$ , respectively).  
292 Pups from the rsvGL and rsvL groups had significantly smaller lesions compared to those in the other  
293 HI groups ( $33 \pm 2\%$  and  $31 \pm 3\%$ , respectively). At P9, pups from the rsvGL group showed the smallest  
294 brain lesion volume compared to the other HI groups ( $9 \pm 2\%$  vs.  $21 \pm 2\%$ ,  $22 \pm 3\%$ ,  $19 \pm 3\%$  and  $16$   
295  $\pm 3\%$  for HIC, rsvG, rsvL and rsvC groups, respectively). At P30, no significant difference was detected  
296 for brain lesion volumes in pups from the HIC, rsvG and rsvL groups ( $25 \pm 4\%$ ,  $17 \pm 4\%$  and  $25 \pm 5\%$ ,  
297 respectively). The smallest brain lesion volumes at P30 were measured in pups whose mother had RSV  
298 supplementation during the last week of gestation + the 1<sup>st</sup> week of lactation (rsvGL group) or during  
299 the lactation period after the HI event (rsvC group) ( $9 \pm 3\%$  and  $9 \pm 3\%$ , respectively).

300 A temporal profile of brain lesion evolution was established (Figure 3D) for each group from P7 to  
301 P30. A decrease in brain lesion volume was detected in all groups within the first 48 hours post-HI due  
302 to the spontaneous recovery of part of the damaged tissue (penumbra without necrosis). The most  
303 extensive recovery was observed for pups in the rsvGL group (mother with the longest RSV  
304 supplementation, before the HI event). No statistical difference was found between P9 and P30, for all  
305 groups.

306 ADC values were measured in the cortex, hippocampus and striatum of all groups (Figure 3E).  
307 Independently of the considered structure, a significant drop in ADC values was detected in all HI  
308 groups compared to sham groups. There was no significant difference between ADC values measured  
309 in HI groups in the cortex, while in the hippocampus, pups from the rsvL group presented slightly but  
310 significantly higher ADC values compared to other HI groups, reflecting a less severe cytotoxic edema.  
311 The same increase in ADC values can be observed in the striatum in pups from rsvGL and rsvL groups  
312 compared to HIC.

313

### 314 ***Maternal RSV supplementation preserves cognitive and sensorimotor functions of pups***

315 Behavioral evaluations of each group are shown in Figure 4. Righting reflex was performed from P8  
316 to P12 (Figure 4A) for pups from sham, HIC, rsvGL, rsvG and rsvL groups. At P8 and P12, pups from  
317 the HIC group took a significantly longer time to turn back on their four paws compared to pups from  
318 the other groups. At P10, pups from all groups (RSV supplemented and sham) except from the rsvG  
319 group performed significantly better than pups from the HIC group. Moreover, there was a statistical  
320 difference between sham pups and pups from the rsvG and rsvL groups, which took a longer time to  
321 turn back on their paws. In addition, at P12, sham pups were significantly better than pups from any of  
322 the RSV groups.

323 Sensorimotor deficits were also assessed using the mNSS test (Figure 4B). While pups in the sham  
324 group showed no impairment (score  $< 1$ ;  $0.6 \pm 0.2$ ), pups in the HIC group had the highest neurological  
325 deficits ( $3.8 \pm 0.4$ ). Concerning pups whose mother received RSV supplementation, their mNSS scores  
326 were better (lower) than pups in the HIC group ( $1.6 \pm 0.1$ ,  $2.7 \pm 0.3$ ,  $1.7 \pm 0.3$  and  $2.5 \pm 0.3$  for pups  
327 from the rsvGL, rsvG, rsvL and rsvC groups, respectively). Among the groups whose mothers were  
328 supplemented with RSV, pups from the rsvGL and rsvL groups presented the best (lowest) scores.

329 Long-term memory was evaluated with the novel object recognition test at P45 (Figure 4C). Pups from  
330 HIC and rsvG groups showed a significantly lower discrimination index than sham pups  
331 (discrimination index:  $0.47 \pm 0.06$  and  $0.48 \pm 0.04$  for HIC and rsvG groups, respectively vs.  $0.76 \pm$   
332  $0.02$  for sham group). No significant difference was detected between sham, rsvGL, and rsvL groups.  
333 Pups from the RsvC group exhibited heterogenous results but a tendency to be like those of the sham,  
334 rsvGL and rsvL groups.

335

336 ***Maternal RSV supplementation induces changes in the expression pattern of cortical genes involved***  
337 ***in sirtuin signaling and intercellular metabolic interactions***

338 Mechanisms involved in short-term cortical neuroprotection by RSV were further evaluated using RT-  
339 qPCR on P9 cortical samples of pups from the rsvGL group (Figure 5; for hippocampus and striatum  
340 data, see supplementary Figure 3 and 4). Putative anti-apoptotic and anti-oxidant effects of RSV  
341 supplementation were assessed by quantification of SIRT1, Bcl2 and SOD2 mRNA expression in both  
342 undamaged and damaged cortical hemispheres (Figure 5A). Possible impact of maternal  
343 supplementation on glutamate uptake and astrocyte-neuron lactate shuttling was explored by  
344 quantification of MCT1, MCT2, LDHa, LDHb, GLAST, GLT1 and Na<sup>+</sup>/K<sup>+</sup>ATPase  $\alpha_2$  subunit mRNA  
345 expression in both undamaged and damaged cortical hemispheres (Figure 5B). Independently of the  
346 considered structure, maternal RSV supplementation significantly enhanced SIRT1 mRNA expression  
347 in both hemispheres (undamaged and damaged hemispheres) compared to sham and HIC groups. In  
348 the cortex, a relative 50% increase in SIRT1 mRNA expression was thus measured in the undamaged  
349 hemisphere compared to the sham group, while a 30% increase was observed in the damaged side. In  
350 contrast, no significant difference for SIRT1 mRNA expression was measured between sham and HIC  
351 groups, neither in the damaged nor in the undamaged hemisphere. Bcl2 mRNA expression also  
352 increased with maternal RSV supplementation in both hemispheres (a relative 62% and 33% increase  
353 was measured compared to sham, in the undamaged and damaged cortex, respectively). The HI event  
354 *per se* did not modulate Bcl2 mRNA expression. In addition, SOD2 mRNA content was higher in the  
355 rsvGL group ( $+31 \pm 6\%$  in the undamaged cortex compared to sham). In the damaged hemisphere, HI  
356 induced a decrease of SOD2 mRNA expression, which was reversed by maternal RSV  
357 supplementation.

358 Concerning genes linked to glutamate transport and lactate shuttling, all (MCT1, MCT2, LDHa, LDHb,  
359 GLT1, GLAST and the Na<sup>+</sup>/K<sup>+</sup> ATPase  $\alpha_2$  subunit) had at least a tendency to increase with the RSV  
360 treatment. In the undamaged hemisphere, increases in mRNA expression were statistically significant  
361 for MCT1 (+31  $\pm$  11%), LDHa (+40  $\pm$  5%), GLAST (+27  $\pm$  8%), GLT1 (+30  $\pm$  6%) and the  
362 Na<sup>+</sup>/K<sup>+</sup>ATPase  $\alpha_2$  subunit (+28  $\pm$  2%) compared to the sham group. In the damaged hemisphere, a  
363 strong decrease in MCT2 mRNA levels was measured in the HIC group vs. the sham group (-80  $\pm$  5%).  
364 This level was partially restored with maternal RSV supplementation. The HI event also reduced the  
365 relative mRNA expression of LDHa and LDHb in the damaged cortex (-41  $\pm$  5% and -39  $\pm$  6%,  
366 respectively, compared to sham group). Once again, RSV counteracted these reductions since no  
367 significant difference was observed in LDHa and LDHb mRNA levels between the rsvGL and sham  
368 groups. When looking at the astrocytic glutamate transporters, RSV increased the relative cortical  
369 GLAST mRNA expression in both hemispheres (relative GLAST expression compared to the sham  
370 group: +27  $\pm$  8% and +66  $\pm$  20% in the undamaged and damaged cortex, respectively). In the  
371 undamaged hemisphere, RSV led to an increase in GLT1 mRNA expression (+30  $\pm$  6%, compared to  
372 sham). While the HI event did not affect GLT1 mRNA levels in the undamaged hemisphere, its  
373 expression was downregulated in the damaged cortex (-70  $\pm$  2%, compared to sham). Maternal RSV  
374 supplementation allowed to restore GLT1 mRNA expression in the damaged cortex. Finally, the  
375 Na<sup>+</sup>/K<sup>+</sup>ATPase  $\alpha_2$  subunit mRNA content was modulated by maternal RSV supplementation in the  
376 undamaged cortex only since its expression was increased (+28  $\pm$  2%, compared to sham group). No  
377 statistical difference was observed between sham and HIC groups concerning the Na<sup>+</sup>/K<sup>+</sup>ATPase  $\alpha_2$   
378 subunit mRNA levels.

379

380 ***Maternal RSV supplementation increases cortical expression of key proteins linked to astrocyte-***  
381 ***neuron lactate shuttle (ANLS).***

382 Results at the mRNA level prompted us to further investigate if the protein expression of key elements  
383 of the ANLS was modified. MCT1 protein expression showed no statistically significant change in  
384 both cortices independently of the condition whereas maternal RSV supplementation partially restored  
385 MCT2 protein expression altered by the HI event only in the damaged hemisphere (Figure 6). This was  
386 not the case for LDHa, which exhibited a drop in protein expression for both damaged and undamaged  
387 cortices that was unaffected by the RSV treatment. However, maternal RSV supplementation increased  
388 LDHb protein levels in both cortices (+99  $\pm$  30% and +146  $\pm$  53 % for undamaged and damaged cortex  
389 compared to sham, respectively) although the HI event had no effect *per se*. Finally, for the astrocytic  
390 glutamate transporter GLAST, HI induced an up-regulation in the undamaged cortex (+96  $\pm$  38%,  
391 compared to sham), which was unaffected by RSV supplementation. In the damaged cortex, only a  
392 non-significant reduction in GLAST protein expression was observed with a tendency to prevent it by  
393 the RSV treatment.

394

395 ***Maternal RSV supplementation reduces neuronal cell death***

396 Typical Nissl staining of cortical brain sections from one representative pup of the sham, HIC and  
397 rsvGL groups are shown Figure 7A (striatum shown in supplementary Figure 5). The presence of Nissl  
398 bodies is widely employed to detect viable neurons. Staining indicated that neurons in the sham group  
399 displayed typical and homogenous morphologies. In the undamaged cortex, HI did not lead to  
400 significant neuronal cell death (Figure 7A and B). On the contrary, in the damaged hemisphere, several

401 neuro-morphological changes were observed after the HI event in pups from the HIC group, with an  
402 increased number of pyknotic neurons and a strong decrease in Nissl body content. The HI event  
403 induced neuronal necrosis and apoptosis, leading to neuronal loss in the cortex of the damaged  
404 hemisphere in pups from the HIC group ( $-81 \pm 4\%$ , in the damaged cortex, Figure 7A and B). In the  
405 brain of pups whose mother received RSV supplementation during the last week of gestation and the  
406 1<sup>st</sup> week of lactation, such a neuronal loss was not observed, even if they underwent the same HI event  
407 compared to pups in the HIC group. No significant difference was detected in terms of the number of  
408 viable neurons between sham and rsvGL groups in the damaged cortex (Figure 7A and B).

409

#### 410 **4 Discussion**

411 Neonatal cerebral HI is an important cause of neonatal death and brain disorders with lasting  
412 deficiencies. Brain HI during the neonatal period leads to well-documented damages of the affected  
413 brain regions due to complex biochemical cascades (Kohlhauser et al., 1999). These activated  
414 processes lead to excitotoxicity, oxidative stress, deficiency in ATP-dependent pumps and cell death.  
415 In this study, we focused on maternal RSV supplementation, using a nutritional dose of RSV (0.15  
416 mg/kg/d), which corresponds to the consumption of about 22 g of grapes (about thirty grape berries)  
417 per day for a pregnant woman (Dumont et al., 2020) and we followed brain lesions in P7-pups related  
418 to a HI event. In the control group (pregnant female without any RSV supplementation), a HI event in  
419 pups induced severe HI lesions, since their volume represented around 40% of the total brain, as already  
420 characterized in this Rice-Vannucci model (Ashwal et al., 2007). Maternal RSV supplementation was  
421 tested during various time-windows (the last week of gestation or/and the first week of lactation  
422 (preventive treatment) or the second week of lactation (curative treatment)). Results indicated that the  
423 best neuroprotective effect was observed with the longest preventive supplementation period (rsvGL  
424 group), as already observed with piceatannol, an analogue of resveratrol (Dumont et al., 2019). Indeed,  
425 MRI measurements at P7, 3h post common carotid artery ligation, revealed a 21%-decrease in brain  
426 lesion volume for pups from the rsvGL group compared to pups from the HIC group.

427

#### 428 *Nutritional approach vs. direct treatment*

429 Several publications have already reported that a direct pretreatment with RSV prevents neuronal  
430 injury. In particular Arteaga *and al.* injected RSV (20mg/kg ; i.p ) in P7-pups just before HI (same  
431 Rice and Vannucci model) and they observed a 80% decrease in lesion volume 7 days after the HI  
432 insult ( $30 \pm 2\%$  for HI group compared to  $5 \pm 1\%$  for RSV treated group 7 days after HI) (Arteaga et  
433 al., 2015). Moreover, Gao *and al.* showed that a daily dose of RSV to pups (low dose 20 mg/kg or high  
434 dose 40 mg/kg; i.p) for one week before HI could reduce the lesion size and cerebral edema in pups.  
435 They observed a reduction of the lesion size around 40% for a low dose of RSV and 50% for a high  
436 dose of RSV 3h post HI insult at P14 (Gao et al., 2018). RSV has neuroprotective effect leading to  
437 functional benefits since, in addition to reduce the number of pups with lesion and decrease the infarct  
438 area, it improves behavioral deficits caused by HI. Indeed, our results showed a better motricity, as  
439 well as memory with RSV treatment, similarly to the results reported by Karalis *and al.* This study  
440 showed that direct administration of RSV to pups (90mg/kg; i.p) immediately after P7-HI significantly  
441 reduces HI-induced brain injury as well as short- and long-term behavioral impairments (Karalis et al.,  
442 2011). Strikingly, 24h after the HI insult, RSV-treated pups exhibited better performance in righting  
443 reflex just like we observed in our experiments.

444 Our study demonstrates a significant RSV neuroprotection that is comparable to the one reported in  
445 the literature in a similar model but by direct treatment of pups. However, our approach is certainly  
446 more likely to be acceptable for a transfer to the clinic since the mode of administration of the treatment  
447 (in dam's drinking water compared to i.p. injection) is less invasive and the dose (our daily dose of  
448 0,15mg/kg compared to around 40mg/kg) is within a reasonable nutritional range. An important point  
449 raised by the comparison between the literature and our results, is that the best results are observed  
450 when RSV is present at the time of the HI event. Indeed, in rsvG (RSV treatment was stopped 7d before  
451 HI insult), the neuroprotection is not as effective as observed for rsvGL or rsv L, suggesting that the  
452 closest to the HI event occurs the supplementation, the more neuroprotective it becomes.

453 A HI insult leads to a deficiency in oxygen and glucose, inducing a decrease in ATP production and  
454 an alteration of all energetically-dependent mechanisms. ATP-dependent pumps are no longer  
455 efficient, which leads to an ionic imbalance and a cellular water influx responsible for cell swelling  
456 and, at a larger scale, to cytotoxic edema (Badaut et al., 2011). ADC values, which decrease during the  
457 first hours after the insult due to water movement restriction linked to the edema, were measured by  
458 DWI, in the three most affected structures (cortex, hippocampus and striatum) (Vannucci et al., 1999).  
459 A decrease in ADC values was measured, as observed in previous studies (Miyasaka et al., 2000;  
460 McKinstry et al., 2002). However, this decrease was slightly lower in the striatum of pups from the  
461 rsvGL and rsvL groups, indicating that cytotoxic edema was less severe. This slight neuroprotective  
462 effect has already been shown in another study, in the same model of P7-HI pups with lactate as  
463 neuroprotective agent (Roumes et al., 2020). This striatal specific neuroprotective effect was also  
464 observed after a middle cerebral artery occlusion in the mouse, since a lactate injection led to a  
465 significant reduction of the lesion size, which was more pronounced in the striatum (Berthet et al.,  
466 2009). Indeed, Berthet *et al.*, in order to understand why lactate protected mainly the striatum,  
467 measured lactate concentrations in each structure after lactate injection in healthy mice by MR  
468 spectroscopy; they showed that the lactate concentration was higher in the striatum (Berthet et al.,  
469 2009). In addition, another study indicated that RSV decreased anoxia-induced dopamine release and  
470 appeared as a promising agent to improve the alterations occurring under anoxic-ischemic conditions  
471 in striatal sections by protecting dopaminergic neurons (Gursoy and Buyukuysal, 2008). Indeed,  
472 dopamine was implicated in the development of an ischemic lesion in the striatum and a reduction of  
473 dopamine release protects this structure against ischemic lesions (Globus et al., 1987).

474

#### 475 ***Correlation between lesion size and behavioral performance***

476 MRI is a powerful technique that allows longitudinal follow-up of animals. Such a non-invasive  
477 technique could thus be coupled with behavioral tests at different ages to correlate with cognitive  
478 performance. Indeed, images alone are not necessarily predictive of brain functions, since rat pups have  
479 high neuronal plasticity, which allows them to spontaneously recover some brain capacities (Wittmann  
480 et al., 2004). Pups from the rsvGL group exhibited the smallest lesion volumes and the best  
481 performance in all tests compared to the other groups. These results are in accordance with a previous  
482 study showing a greater reduction in brain damages and a preservation of behavioral abilities after  
483 maternal piceatannol (a RSV analogue) supplementation during gestation and breastfeeding than  
484 during breastfeeding alone (Dumont et al., 2019). Interestingly, pups from the rsvL group showed the  
485 same performance level than sham pups and pups from the rsvGL pups in behavioral tests, while their  
486 brain lesion volumes were bigger than the one measured in pups from the rsvGL group (at any time  
487 point), and not statistically different from the brain lesion volumes of pups from the control group  
488 (HIC). These results clearly indicate that (i) MRI alone just after the insult may not be accurately

489 predictive of eventual brain function impairments and (ii) behavioral tests are necessary to evaluate the  
490 potential neuroprotection of a tested treatment. Concerning the time-window for maternal RSV  
491 supplementation, data (MRI and behavior) indicated that when the RSV supplementation was stopped  
492 one week before the neonatal HI event, the neuroprotective effect was the lowest. When RSV was  
493 present only during the last week of gestation (rsvG), pups displayed a significant decrease in lesion  
494 size only at P30 and minimal recovery of short-term behavioral performances (righting reflex and  
495 mNSS scores). However, this neuroprotection was not sufficient to protect the hippocampus since long-  
496 term memory was not preserved. These data could be explained by the fact that the CA1 area of the  
497 hippocampus is usually the most vulnerable structure, followed by the neocortex and then by the  
498 striatum (Smith et al., 1984).

499

500 Although maternal RSV supplementation administered before the HI event in pups was  
501 neuroprotective, we also wanted to test its potential curative effect. Therefore, a rsvC group was  
502 created, in which RSV was present in the drinking water of the breastfeeding female just after the  
503 neonatal HI insult. Interestingly, even if administered after the HI insult, pups from the rsvC group had  
504 better mNSS scores and performed better in the novel object recognition test than pups from the HIC  
505 group. Such a curative effect of resveratrol was also observed in the same context but with a direct  
506 treatment (Pan et al., 2016). Indeed, 3 doses of RSV (100mg/kg; i.p) in the post-HI P7 pup model at  
507 0h, 8h and 18h reduced both the lesion size, as well as the expression levels of key inflammatory factors  
508 and pro-apoptotic molecules 7 days after. These data confirm that MRI alone just after the insult is not  
509 a predictive technique of the sensory-cognitive-motor functions and (ii) that it is necessary to evaluate  
510 the effectiveness of a therapeutic approach using a long-term evaluation.

511

### 512 ***Putative molecular mechanisms involved in neuroprotective effects***

513 To further understand the basis of these effects, we aimed at deciphering the molecular mechanisms  
514 involved in RSV neuroprotection. For this purpose, only pup's brains from the most effective  
515 supplementation regimen (pups from the rsvGL group) were analyzed in parallel with sham and HIC  
516 groups. As a first step, we focused on some targets from a signaling pathway which is known to be  
517 regulated by RSV (SIRT1 (Lagouge et al., 2006), SOD (Toader et al., 2013), Bcl2 (Pan et al., 2016)).  
518 HI is characterized by two consecutive traumatic events: HI itself and the reperfusion period, which  
519 induces oxidative stress and ROS production (Ten and Starkov, 2012). This increase in oxidative stress  
520 leads to a dysfunction of the Na<sup>+</sup>/K<sup>+</sup>-ATPase, then brain edema and blood-brain barrier disruption  
521 (Himadri et al., 2010). The Na<sup>+</sup>/K<sup>+</sup>-ATPase plays a major role in the maintenance of intracellular  
522 electrolyte homeostasis and has been shown to be particularly sensitive to ROS-induced damages  
523 (Lima et al., 2009). In response to this insult, SOD, by stimulating the conversion of superoxide to  
524 hydrogen peroxide, is one of the main antioxidant defense systems to scavenge ROS (Wang et al.,  
525 2018). Studies have described that the expression of SOD is regulated by SIRT1 through deacetylation  
526 of the transcription factor FoxO3a and the transcriptional coactivator peroxisome proliferator-activated  
527 receptor  $\gamma$ -coactivator 1 $\alpha$  (PGC-1 $\alpha$ ) (Olmos et al., 2013). In our model, the neonatal HI insult induced  
528 a decrease in SOD expression, which was partially counteracted by maternal RSV supplementation  
529 which also enhanced SIRT1 levels. Our results agree with previous data reported by Shin *et al.* who  
530 showed that RSV protected from ischemic stroke by upregulating the SIRT1-PGC-1 $\alpha$  signaling  
531 pathway leading to an antioxidant effect under ischemic stress (Shin et al., 2012). In another study,  
532 using a P14-neonatal rat HI model, direct pre-treatment with RSV (20 or 40 mg/kg, for seven

533 consecutive days before HI induction) was shown to alleviate oxidative stress, in part by increasing  
534 SOD expression just after the HI event (Gao et al., 2018). Likewise, in an adult rat model of transient  
535 global cerebral ischemia, it has been reported that RSV (30 mg/kg; i.p injections 7 d prior to ischemia)  
536 is neuroprotective and restores  $\text{Na}^+/\text{K}^+$ -ATPase activity in the cortex and hippocampus back to normal  
537 levels (Simao et al., 2011). Activation of SIRT1 signaling during neonatal HI by RSV was paralleled  
538 by an increased expression of Bcl2. A SIRT1-dependent increase in Bcl2 has also been reported in a  
539 stroke context after curcumin pretreatment and has been linked to anti-inflammatory properties (Miao  
540 et al., 2016). Similarly, in oxygen–glucose deprivation (OGD) injury models, an upregulation of SIRT1  
541 caused an increased expression of the anti-apoptotic Bcl2 and a decreased expression of the pro-  
542 apoptotic cleaved caspase-3 (Yan et al., 2013). In our study, the increase of SIRT1, Bcl2 and SOD2  
543 expression was confirmed, as shown in previous studies which explored the direct impact of RSV.  
544 These data confirm that our transgenerational and nutritional approach is as effective as a direct  
545 treatment and that similar upregulations of SIRT1, Bcl2 and SOD2 are observed in pup's brains when  
546 RSV was administered to the mother compared to a direct administration.

547 In a second step, we looked at the potential impact of maternal RSV supplementation on neonatal brain  
548 metabolism. Indeed, only a few studies have investigated the effect of RSV on cerebral metabolism  
549 under physiological or pathological conditions, and none looked at it in a transgenerational context. In  
550 one study, it was observed first that transient forebrain ischemia in adult rat led to a decrease in GLT1  
551 expression (Girbovan and Plamondon, 2015), the major astrocytic glutamate transporter. The decrease  
552 in astrocytic glutamate uptake induced by HI is responsible for glutamatergic excitotoxicity, which is  
553 a major cause of neuronal death. This decrease was reversed by RSV pretreatment (1 or 10 mg/kg dose;  
554 i.p.) (Girbovan and Plamondon, 2015). In our model, HI also induced a decrease in astrocytic GLT1  
555 mRNA content in the damaged hemisphere, which was counteracted by maternal RSV  
556 supplementation. GLAST mRNA content was not downregulated by the neonatal HI event, but was  
557 upregulated by maternal RSV treatment (in both hemispheres). This upregulation of glutamate  
558 transporter mRNA expression by RSV may lead to a decrease in glutamatergic excitotoxicity  
559 promoting neuronal survival, as confirmed by Nissl staining. Astrocytic glutamate uptake is also  
560 implicated in astrocyte-neuron metabolic interactions. Indeed, astrocytic glutamate reuptake  
561 ( $3\text{Na}^+/\text{glutamate}$  co-transport) after neuronal activity has been shown to activate astrocytic glycolysis  
562 (through the  $\text{Na}^+/\text{K}^+$ -ATPase activation, which excludes  $\text{Na}^+$ ) and lactate production, which is  
563 transferred to neurons and used as a neuronal oxidative fuel (Pellerin and Magistretti, 1994). This  
564 lactate shuttling process is named ANLS for astrocyte-neuron lactate shuttle. Lactate is shuttled from  
565 astrocytes to neurons *via* monocarboxylate transporters (MCTs), with different isoforms exhibiting a  
566 preferential cellular localization (MCT2 on neurons, MCT1 on astrocytes and endothelial cells). In  
567 previous studies, we have shown that i) RSV can activate glycolysis (*ex vivo* NMR spectroscopy study  
568 on perfused liver) (Beauvieux et al., 2013) and, more recently, ii) that lactate is neuroprotective after a  
569 neonatal HI event (Roumes et al., 2020). Taken altogether, our results led us to hypothesize that RSV  
570 supplementation, in addition to classical signaling pathways, may impact other metabolic pathways,  
571 and more particularly can modulate the ANLS. This hypothesis is supported by the increase in mRNA  
572 levels of the key elements involved in the ANLS: the MCTs, the lactate dehydrogenase (LDH) isoforms  
573 (that converts pyruvate into lactate and *vice versa*), the astrocytic glutamate transporters (GLAST and  
574 GLT1) and the  $\alpha_2$  subunit of the  $\text{Na}^+/\text{K}^+$ -ATPase. In the context of HI, during the latent phase, lactate  
575 may act as an alternative fuel to counteract the energy deficit that occurred during the HI event. This  
576 is consistent with the increased expression of the LDHb isoform (which favors the conversion of lactate  
577 into pyruvate and therefore favors lactate consumption) at the protein level, and not the LDHa isoform  
578 (which favors pyruvate into lactate conversion, and therefore favors lactate production). There is a  
579 selective distribution of these two subunits of LDH, the isoenzyme LDH-5 (4 LDHa subunits) is more  
580 present in glycolytic tissues while the isoenzyme LDH-1 (4 LDHb subunits) is more predominant in

581 oxidative tissues (Markert et al., 1975). Another study has shown that neurons have a strong content in  
582 LDHb-enriched isoenzymes while astrocytes have more LDHa-enriched isoenzymes (Bittar et al.,  
583 1996). These observations suggested a regulated lactate flux between astrocytes and neurons which  
584 was recently demonstrated *in vivo* (Machler et al., 2016). These data reinforced the concept that  
585 astrocytes actively produce and release lactate that is subsequently transferred to neurons as an  
586 energetic substrate to be used in the tricarboxylic acid cycle (TCA). The metabolic use of lactate as an  
587 energetic substrate for neurons allows to spare glucose for other important cellular repair mechanisms,  
588 such as the pentose phosphate pathway (PPP), which activity is crucial for the production of glutathione  
589 or ROS scavenger particularity for the neonates (Morken et al., 2014). PPP has a critical role in  
590 neuronal survival during cerebral ischemia/reperfusion as it produces crucial antioxidant molecules in  
591 order to reduce the oxidative stress and inflammation (Cao et al., 2017).

592

### 593 **Conclusion**

594 A summary of all modulations observed in this study is provided schematically in Figure 8. Maternal  
595 supplementation with RSV alleviates the negative impact of inflammatory, apoptotic and ROS  
596 pathways in a context of neonatal HI. Furthermore, RSV modulates brain metabolism by upregulating  
597 some key components of the ANLS. *In fine*, RSV promotes neuronal survival, and, more importantly,  
598 preserves motor and cognitive abilities. The originality of this study was to combine different  
599 techniques (MRI, behavioral investigations, histology, gene and protein expression analyses) to  
600 characterize brain lesions and their functional consequences, and to decipher the molecular  
601 mechanisms behind this neuroprotection. Of note, our proposed nutritional and transgenerational  
602 approach to administer RSV could be of great interest in the search for a realistic and easily  
603 implementable neuroprotective strategy against the deleterious effects induced by neonatal HI.

604

### 605 **5 References**

606 Neonatal cerebral HI is an important cause of neonatal death and brain disorders with lasting  
607 deficiencies. Arteaga, O., Revuelta, M., Uriguen, L., Alvarez, A., Montalvo, H., and Hilario, E., 2015.  
608 Pretreatment with Resveratrol Prevents Neuronal Injury and Cognitive Deficits Induced by Perinatal  
609 Hypoxia-Ischemia in Rats. PLoS One 10, e0142424.

610 Ashwal, S., Tone, B., Tian, H. R., Chong, S., and Obenaus, A., 2007. Comparison of two neonatal  
611 ischemic injury models using magnetic resonance imaging. *Pediatr Res* 61, 9-14.

612 Badaut, J., Ashwal, S., and Obenaus, A., 2011. Aquaporins in cerebrovascular disease: a target for  
613 treatment of brain edema? *Cerebrovasc Dis* 31, 521-531.

614 Baur, J. A., and Sinclair, D. A., 2006. Therapeutic potential of resveratrol: the *in vivo* evidence. *Nat*  
615 *Rev Drug Discov* 5, 493-506.

616 Beauvieux, M. C., Stephant, A., Gin, H., Serhan, N., Couzigou, P., and Gallis, J. L., 2013. Resveratrol  
617 mainly stimulates the glycolytic ATP synthesis flux and not the mitochondrial one: a saturation transfer  
618 NMR study in perfused and isolated rat liver. *Pharmacol Res* 78, 11-17.

- 619 Berthet, C., Lei, H., Thevenet, J., Gruetter, R., Magistretti, P. J., and Hirt, L., 2009. Neuroprotective  
620 role of lactate after cerebral ischemia. *J Cereb Blood Flow Metab* 29, 1780-1789.
- 621 Bian, H., Shan, H., and Chen, T., 2017. Resveratrol ameliorates hypoxia/ischemia-induced brain injury  
622 in the neonatal rat via the miR-96/Bax axis. *Childs Nerv Syst* 33, 1937-1945.
- 623 Bittar, P. G., Charnay, Y., Pellerin, L., Bouras, C., and Magistretti, P. J., 1996. Selective distribution  
624 of lactate dehydrogenase isoenzymes in neurons and astrocytes of human brain. *J Cereb Blood Flow*  
625 *Metab* 16, 1079-1089.
- 626 Bona, E., Hagberg, H., Loberg, E. M., Bagenholm, R., and Thoresen, M., 1998. Protective effects of  
627 moderate hypothermia after neonatal hypoxia-ischemia: short- and long-term outcome. *Pediatr Res* 43,  
628 738-745.
- 629 Bourque, S. L., Dolinsky, V. W., Dyck, J. R., and Davidge, S. T., 2012. Maternal resveratrol treatment  
630 during pregnancy improves adverse fetal outcomes in a rat model of severe hypoxia. *Placenta* 33, 449-  
631 452.
- 632 Cao, L., Zhang, D., Chen, J., Qin, Y. Y., Sheng, R., Feng, X., Chen, Z., Ding, Y., Li, M., and Qin, Z.  
633 H., 2017. G6PD plays a neuroprotective role in brain ischemia through promoting pentose phosphate  
634 pathway. *Free Radic Biol Med* 112, 433-444.
- 635 Das, S., and Das, D. K., 2007. Anti-inflammatory responses of resveratrol. *Inflamm Allergy Drug*  
636 *Targets* 6, 168-173.
- 637 Dumont, U., Sanchez, S., Olivier, B., Chateil, J. F., Deffieux, D., Quideau, S., Pellerin, L., Beauvieux,  
638 M. C., Bouzier-Sore, A. K., and Roumes, H., 2020. Maternal alcoholism and neonatal hypoxia-  
639 ischemia: Neuroprotection by stilbenoid polyphenols. *Brain Res* 1738, 146798.
- 640 Dumont, U., Sanchez, S., Olivier, B., Chateil, J. F., Pellerin, L., Beauvieux, M. C., Bouzier-Sore, A.  
641 K., and Roumes, H., 2019. Maternal consumption of piceatannol: A nutritional neuroprotective  
642 strategy against hypoxia-ischemia in rat neonates. *Brain Res* 1717, 86-94.
- 643 Ennaceur, A., and Delacour, J., 1988. A new one-trial test for neurobiological studies of memory in  
644 rats. 1: Behavioral data. *Behav Brain Res* 31, 47-59.
- 645 Gao, Y., Fu, R., Wang, J., Yang, X., Wen, L., and Feng, J., 2018. Resveratrol mitigates the oxidative  
646 stress mediated by hypoxic-ischemic brain injury in neonatal rats via Nrf2/HO-1 pathway. *Pharm Biol*  
647 *Sci* 56, 440-449.
- 648 Girbovan, C., and Plamondon, H., 2015. Resveratrol downregulates type-1 glutamate transporter  
649 expression and microglia activation in the hippocampus following cerebral ischemia reperfusion in  
650 rats. *Brain Res* 1608, 203-214.
- 651 Globus, M. Y., Ginsberg, M. D., Dietrich, W. D., Busto, R., and Scheinberg, P., 1987. Substantia nigra  
652 lesion protects against ischemic damage in the striatum. *Neurosci Lett* 80, 251-256.
- 653 Gluckman, P. D., Wyatt, J. S., Azzopardi, D., Ballard, R., Edwards, A. D., Ferriero, D. M., Polin, R.  
654 A., Robertson, C. M., Thoresen, M., Whitelaw, A., and Gunn, A. J., 2005. Selective head cooling with

- 655 mild systemic hypothermia after neonatal encephalopathy: multicentre randomised trial. *Lancet* 365,  
656 663-670.
- 657 Gursoy, M., and Buyukuysal, R. L., 2008. Resveratrol protects rat striatal slices against anoxia-induced  
658 dopamine release. *Neurochem Res* 33, 1838-1844.
- 659 Himadri, P., Kumari, S. S., Chitharanjan, M., and Dhananjay, S., 2010. Role of oxidative stress and  
660 inflammation in hypoxia-induced cerebral edema: a molecular approach. *High Alt Med Biol* 11, 231-  
661 244.
- 662 Karalis, F., Soubasi, V., Georgiou, T., Nakas, C. T., Simeonidou, C., Guiba-Tziampiri, O., and  
663 Spandou, E., 2011. Resveratrol ameliorates hypoxia/ischemia-induced behavioral deficits and brain  
664 injury in the neonatal rat brain. *Brain Res* 1425, 98-110.
- 665 Kohlhauser, C., Kaehler, S., Mosgoeller, W., Singewald, N., Kouvelas, D., Prast, H., Hoeger, H., and  
666 Lubec, B., 1999. Histological changes and neurotransmitter levels three months following perinatal  
667 asphyxia in the rat. *Life Sci* 64, 2109-2124.
- 668 Kurinczuk, J. J., White-Koning, M., and Badawi, N., 2010. Epidemiology of neonatal encephalopathy  
669 and hypoxic-ischaemic encephalopathy. *Early Hum Dev* 86, 329-338.
- 670 Lagouge, M., Argmann, C., Gerhart-Hines, Z., Meziane, H., Lerin, C., Daussin, F., Messadeq, N.,  
671 Milne, J., Lambert, P., Elliott, P., Geny, B., Laakso, M., Puigserver, P., and Auwerx, J., 2006.  
672 Resveratrol improves mitochondrial function and protects against metabolic disease by activating  
673 SIRT1 and PGC-1alpha. *Cell* 127, 1109-1122.
- 674 Lima, F. D., Oliveira, M. S., Furian, A. F., Souza, M. A., Rambo, L. M., Ribeiro, L. R., Silva, L. F.,  
675 Retamoso, L. T., Hoffmann, M. S., Magni, D. V., Pereira, L., Figuera, M. R., Mello, C. F., and Royes,  
676 L. F., 2009. Adaptation to oxidative challenge induced by chronic physical exercise prevents Na<sup>+</sup>,K<sup>+</sup>-  
677 ATPase activity inhibition after traumatic brain injury. *Brain Res* 1279, 147-155.
- 678 Mächler, P., Wyss, M. T., Elsayed, M., Stobart, J., Gutierrez, R., von Faber-Castell, A., Kaelin, V.,  
679 Zuend, M., San Martin, A., Romero-Gomez, I., Baeza-Lehnert, F., Lengacher, S., Schneider, B. L.,  
680 Aebischer, P., Magistretti, P. J., Barros, L. F., and Weber, B., 2016. In Vivo Evidence for a Lactate  
681 Gradient from Astrocytes to Neurons. *Cell Metab* 23, 94-102.
- 682 Markert, C. L., Shaklee, J. B., and Whitt, G. S., 1975. Evolution of a gene. Multiple genes for LDH  
683 isozymes provide a model of the evolution of gene structure, function and regulation. *Science* 189,  
684 102-114.
- 685 McKinstry, R. C., Miller, J. H., Snyder, A. Z., Mathur, A., Schefft, G. L., Almlí, C. R., Shimony, J. S.,  
686 Shiran, S. I., and Neil, J. J., 2002. A prospective, longitudinal diffusion tensor imaging study of brain  
687 injury in newborns. *Neurology* 59, 824-833.
- 688 Miao, Y., Zhao, S., Gao, Y., Wang, R., Wu, Q., Wu, H., and Luo, T., 2016. Curcumin pretreatment  
689 attenuates inflammation and mitochondrial dysfunction in experimental stroke: The possible role of  
690 Sirt1 signaling. *Brain Res Bull* 121, 9-15.

- 691 Miyasaka, N., Nagaoka, T., Kuroiwa, T., Akimoto, H., Haku, T., Kubota, T., and Aso, T., 2000.  
692 Histopathologic correlates of temporal diffusion changes in a rat model of cerebral hypoxia/ischemia.  
693 AJNR Am J Neuroradiol 21, 60-66.
- 694 Morken, T. S., Brekke, E., Haberg, A., Wideroe, M., Brubakk, A. M., and Sonnewald, U., 2014.  
695 Neuron-astrocyte interactions, pyruvate carboxylation and the pentose phosphate pathway in the  
696 neonatal rat brain. Neurochem Res 39, 556-569.
- 697 Morris, D. C., Chopp, M., Zhang, L., Lu, M., and Zhang, Z. G., 2010. Thymosin beta4 improves  
698 functional neurological outcome in a rat model of embolic stroke. Neuroscience 169, 674-682.
- 699 Nnam, N. M., 2015. Improving maternal nutrition for better pregnancy outcomes. Proc Nutr Soc 74,  
700 454-459.
- 701 Olmos, Y., Sanchez-Gomez, F. J., Wild, B., Garcia-Quintans, N., Cabezudo, S., Lamas, S., and  
702 Monsalve, M., 2013. SirT1 regulation of antioxidant genes is dependent on the formation of a  
703 FoxO3a/PGC-1alpha complex. Antioxid Redox Signal 19, 1507-1521.
- 704 Pan, S., Li, S., Hu, Y., Zhang, H., Liu, Y., Jiang, H., Fang, M., Li, Z., Xu, K., Zhang, H., Lin, Z., and  
705 Xiao, J., 2016. Resveratrol post-treatment protects against neonatal brain injury after hypoxia-  
706 ischemia. Oncotarget 7, 79247-79261.
- 707 Pellerin, L., and Magistretti, P. J., 1994. Glutamate uptake into astrocytes stimulates aerobic glycolysis:  
708 a mechanism coupling neuronal activity to glucose utilization. Proc Natl Acad Sci U S A 91, 10625-  
709 10629.
- 710 Rice, J. E., 3rd, Vannucci, R. C., and Brierley, J. B., 1981. The influence of immaturity on hypoxic-  
711 ischemic brain damage in the rat. Ann Neurol 9, 131-141.
- 712 Roumes, H., Dumont, U., Sanchez, S., Mazuel, L., Blanc, J., Raffard, G., Chateil, J. F., Pellerin, L.,  
713 and Bouzier-Sore, A. K., 2020. Neuroprotective role of lactate in rat neonatal hypoxia-ischemia. J  
714 Cereb Blood Flow Metab 271678X20908355.
- 715 Sawda, C., Moussa, C., and Turner, R. S., 2017. Resveratrol for Alzheimer's disease. Ann N Y Acad  
716 Sci 1403, 142-149.
- 717 Shankaran, S., 2012. Hypoxic-ischemic encephalopathy and novel strategies for neuroprotection. Clin  
718 Perinatol 39, 919-929.
- 719 Shin, J. A., Lee, K. E., Kim, H. S., and Park, E. M., 2012. Acute resveratrol treatment modulates  
720 multiple signaling pathways in the ischemic brain. Neurochem Res 37, 2686-2696.
- 721 Simao, F., Matte, A., Matte, C., Soares, F. M., Wyse, A. T., Netto, C. A., and Salbego, C. G., 2011.  
722 Resveratrol prevents oxidative stress and inhibition of Na(+)-K(+)-ATPase activity induced by transient  
723 global cerebral ischemia in rats. J Nutr Biochem 22, 921-928.
- 724 Smith, M. L., Auer, R. N., and Siesjo, B. K., 1984. The density and distribution of ischemic brain injury  
725 in the rat following 2-10 min of forebrain ischemia. Acta Neuropathol 64, 319-332.

- 726 Ten, V. S., and Starkov, A., 2012. Hypoxic-ischemic injury in the developing brain: the role of reactive  
727 oxygen species originating in mitochondria. *Neurol Res Int* 2012, 542976.
- 728 Toader, A. M., Filip, A., Decea, N., and Muresan, A., 2013. Neuroprotective strategy in an  
729 experimental newborn rat model of brain ischemia and hypoxia: effects of Resveratrol and  
730 hypothermia. *Clujul Med* 86, 203-207.
- 731 Vannucci, R. C., Connor, J. R., Mauger, D. T., Palmer, C., Smith, M. B., Towfighi, J., and Vannucci,  
732 S. J., 1999. Rat model of perinatal hypoxic-ischemic brain damage. *J Neurosci Res* 55, 158-163.
- 733 Wang, Y., Branicky, R., Noe, A., and Hekimi, S., 2018. Superoxide dismutases: Dual roles in  
734 controlling ROS damage and regulating ROS signaling. *J Cell Biol* 217, 1915-1928.
- 735 West, T., Atzeva, M., and Holtzman, D. M., 2007. Pomegranate polyphenols and resveratrol protect  
736 the neonatal brain against hypoxic-ischemic injury. *Dev Neurosci* 29, 363-372.
- 737 Wittmann, M., Burtscher, A., Fries, W., and von Steinbuchel, N., 2004. Effects of brain-lesion size and  
738 location on temporal-order judgment. *Neuroreport* 15, 2401-2405.
- 739 Wu, Y. W., and Gonzalez, F. F., 2015. Erythropoietin: a novel therapy for hypoxic-ischaemic  
740 encephalopathy? *Dev Med Child Neurol* 57 Suppl 3, 34-39.
- 741 Yan, W., Fang, Z., Yang, Q., Dong, H., Lu, Y., Lei, C., and Xiong, L., 2013. SirT1 mediates hyperbaric  
742 oxygen preconditioning-induced ischemic tolerance in rat brain. *J Cereb Blood Flow Metab* 33, 396-  
743 406.

744

745 **Tables**

746

Genes	Forward 5'-3'	Reverse 5'-3'
RPS29	GGCTTTTAGGATGGAAGGGAC	TGAAGGTGACAGCAGTCGGTTG
SIRT1	CATACTCGCCACCTAACCTAT	AACCTCTGCCTCATCTACATT
Bcl2	GAGTACCTGAACCGGCATCT	GAAATCAAACAGAGGTCGCA
SOD2	GAGCAAGGTCGCTTACAGA	CTCCCCAGTTGATTACATTC
MCT1	CTTGTGGCGTGATCCT	GTTTCGGATGTCTCGGG
MCT2	GCTCCGTATGCTAAGGAC	CGATAGTGACGAGCCC
GLT1	GAGCATTGGTGCAGCCAGTATT	GTTCTCATTCTATCCAGCAGCCAG
GLAST	CATCCAGGCCAACGAAACA	GAGTCTCCATGGCCTCTGACA
Na <sup>+</sup> /K <sup>+</sup> ATPase	TGTGATTCTGGCTGAGAACG	CAAGTCAGCCCACTGCACTA
LDHa	TGGCCTCTCCGTGGCAGACT	CCCCCAGACCACCTCAACACAA
LDHb	AGACTGCCGTCCCGAACAA	ATCCACCAGGGCAAGCTCA

747

748 **Table 1:** Forward and reverse oligonucleotide sequences of target gene primers for RPS 29, SIRT1,  
 749 Bcl2, SOD2, MCT1, MCT2, GLT1, GLAST, Na<sup>+</sup>/K<sup>+</sup>ATPase, LDHa and LDHb. The specificity of  
 750 oligonucleotide primers was verified using the program BLAST (National Center for Biotechnology  
 751 Information, Bethesda, MD, USA).

752

Anticorps	Sources	Identifier
Rabbit anti-MCT1	Homemade	Riderer Characterized in <a href="#">Pierre et al. (2000)</a>
Rabbit anti-MCT2	Homemade	Riderer Characterized in <a href="#">Pierre et al. (2000)</a>
Rabbit anti-LDHa	Cell signaling	2012S
Rabbit anti-LDHb	Sigma-Aldrich	AV48210
Rabbit anti-GLAST	Abcam	ab416

753

754 **Table 2:** List of antibodies for western blotting

755

## 756 6 Figure legends

### 757 **Figure 1. Composition of experimental groups with different RSV regimens**

758 Seven groups were studied: sham (water without any supplementation for the mother; no HI event for  
 759 the pups), shamrsv (0.15mg/kg/day of RSV in the drinking water of the mother during last week of  
 760 gestation + 1<sup>st</sup> week of lactation; no HI event for pups), HIC (water; HI at P7), rsvGL (0.15mg/kg/day  
 761 of RSV during last week of gestation + 1<sup>st</sup> week of lactation; HI at P7), rsvG (0.15mg/kg/day of RSV  
 762 during last week of gestation; HI at P7), rsvL (0.15mg/kg/day of RSV during 1<sup>st</sup> week of lactation; HI  
 763 at P7), rsvC (0.15mg/kg/day of RSV during 1 week after HI; HI at P7).

764

### 765 **Figure 2. Experimental design**

766 At post-natal day 7 (P7), the left common carotid artery was permanently ligated. Pups were exposed  
 767 to a hypoxic environment (8% oxygen, 33°C, 2 h). MRI acquisitions were performed at P7, P9 and  
 768 P30. Behavioral tests were performed at different time points: righting reflex at P8, P10 and P12; mNSS  
 769 at P24 and novel object recognition test from P41 to P45. Some brains were collected for mRNA and  
 770 protein analysis at P9.

771

772 **Figure 3. Visualization and quantification of brain lesion size with or without RSV treatment**  
 773 **after a HI event**

774 (A) Percentage of P7 pups with brain lesion for HIC, rsvGL, rsvG, rsvL and rsvC groups, 3 h after  
 775 injury. Pups with brain lesion volume < 1% of the total brain volume were considered without brain  
 776 lesion. (B) Typical DW trace images at P7 (top) and T2 images at P30 (bottom) of pup brains for HIC,  
 777 rsvGL, rsvG, rsvL and rsvC groups, acquired on a 4.7T magnet. DW Images were systematically  
 778 acquired 3h after common carotid artery ligation. Damage appeared as a hyposignal at P7 (decrease in  
 779 ADC values due to the edema and cell swelling) and as a hypersignal at P30 (necrotic zone, water and  
 780 cell death). (C) Lesion volumes (% total brain volume) at P7 (3h after the common carotid artery  
 781 ligation; n=31, n=12, n=15, n=13 and n=15 for HIC, rsvGL, rsvG, rsvL and rsvC groups, respectively),  
 782 at P9 (48h after the HI event; n=25, n=14, n=13, n=14 and n=12 for HIC, rsvGL, rsvG, rsvL and rsvC  
 783 groups, respectively) and P30 (23 days after the HI event; n=22, n=13, n=12, n=13 and n=12 for HIC,  
 784 rsvGL, rsvG, rsvL and rsvC groups, respectively). (D) Evolution of lesion volumes as a function of  
 785 time (% relative to lesion volume at P7 for each pup). (E) ADC values (mm<sup>2</sup>/s) in cortical, hippocampal  
 786 and striatal lesions at P7. Results are mean values ± SEM. C, D and E one-way analysis of variance  
 787 (ANOVA) with Fisher's LSD post-hoc test. \*: Significant difference between two groups (\*: p < 0.05,  
 788 \*\*: p < 0.01, \*\*\*: p < 0.001 and \*\*\*\*: p < 0.0001).

789

790 **Figure 4. Behavioral investigations in animals with or without RSV treatment after a HI event**

791 (A) Righting reflex for sham, HIC rsvGL, rsvG, rsvL groups (n=23, n=20, n=17, n=12 and n=15 for  
 792 sham, HIC, rsvGL, rsvG and rsvL groups, respectively) at P8, P10 and P12. (B) mNSS score at P24  
 793 for sham, HIC, rsvGL, rsvG, rsvL and rsvC groups (n= 14, n= 13, n=17, n=13, n=15 and n= 13 for  
 794 sham, HIC, rsvGL, rsvG, rsvL and rsvC groups, respectively). Scoring between 0 and 18 points with:  
 795 <1, no impairment; 1-6, moderate impairment; 7-12, impairment and 13-18, severe impairment. \*:  
 796 different from the HIC group (\*\*: p < 0.01), +: different from the sham group (+: p < 0.05, ++: p <  
 797 0.01) and #: different from the rsvGL (p < 0.05). (C) Discrimination index of the novel object  
 798 recognition test (performed at P45) for sham, HIC, rsvGL, rsvG, rsvL and rsvC groups (n=17, n=17,  
 799 n=13, n=10, n=14 and n=11, respectively). Results are mean values ± SEM; one-way analysis of  
 800 variance (ANOVA) with Fisher's LSD post-hoc test. \*: Significant difference between two groups (\*:  
 801 p < 0.05, \*\*: p < 0.01 and \*\*\*\*: p < 0.0001).

802

803 **Figure 5. Impact of maternal RSV supplementation on cortical expression of some mRNAs**  
 804 **linked to signaling or metabolism**

805 RT-qPCR performed at P9 on cortical samples from damaged and undamaged hemispheres of sham,  
 806 rsvGL and HIC groups (n=6 for each group, hippocampus and striatum (supplementary Figure 3 and  
 807 4). (A) Signaling pathway: SIRT1, Bcl2 and SOD2 mRNA levels were quantified using appropriate  
 808 primer sequences (see Table 1). (B) Metabolic pathway: MCT1, MCT2, LDHa, LDHb, GLAST, GLT1  
 809 and Na<sup>+</sup>/K<sup>+</sup>-ATPase α<sub>2</sub> subunit mRNA levels were quantified using appropriate primer sequences (see  
 810 Table 1). Results are mean values ± SEM and one-way analysis of variance (ANOVA) with Fisher's  
 811 LSD post-hoc test. \*: Significant difference between two groups (\*: p < 0.05, \*\*: p < 0.01, \*\*\*: p <  
 812 0.001 and \*\*\*\*: p < 0.0001).

813

**814 Figure 6. Impact of maternal RSV supplementation on expression of key ANLS proteins**

815 Cortical expression levels of MCT1, MCT2, LDHa, LDHb, GLAST, GLT1 and the Na<sup>+</sup>/K<sup>+</sup>-ATPase  
816  $\alpha_2$  subunit proteins were quantified by Western blots (n=6 for each group). Quantifications were  
817 normalized to Memcode staining. Results are mean values  $\pm$  SEM and one-way analysis of variance  
818 (ANOVA) with Fisher's LSD post-hoc test. \*: Significant difference between two groups (\*: p < 0.05,  
819 \*\*: p < 0.01 and \*\*\*\*: p < 0.0001).

820

**821 Figure 7. Evaluation of neuronal cell death with or without RSV treatment after a HI event**

822 Nissl staining on 16 $\mu$ m-thick cortical brain sections. (A) Percentage of neuronal cell death for sham,  
823 HIC and rsvGL groups in either undamaged or damaged cortex (n=6). Results are mean values  $\pm$  SEM,  
824 one-way analysis of variance (ANOVA) with Fisher's LSD post-hoc test. \*: Significant difference  
825 between two groups (\*\*\*\*: p < 0.0001). (B) Cortical section of a sham control pup, which shows the  
826 normal architecture with many Nissl bodies. Several neuro-morphological changes are observed in the  
827 pup from the HIC group, with increased numbers of pyknotic neurons (dead neurons) and less Nissl  
828 bodies. Maternal RSV supplementation increased the number of Nissl bodies (viable neurons).  
829 Magnification  $\times$ 20; scale bar: 100  $\mu$ m.

830

**831 Figure 8. Summary scheme of maternal RSV neuroprotection on HI damages.**

832 Scheme explaining (i) the deleterious effect of HI on each targeted gene and (ii) the beneficial effects  
833 of maternal RSV supplementation on the three main pathways (anti-apoptotic, anti-oxidant and  
834 metabolic pathway).

835

**836 7 Conflict of Interest**

837 The authors declare that the research was conducted in the absence of any commercial or financial  
838 relationships that could be construed as a potential conflict of interest.

839

**840 8 Author Contributions**

841 UD has acquired and analyzed data, and has contributed to the final drafting of the article. SS has  
842 produced the HI neonate model. CR has participated to Western-Blot and RTqPCR experiments. MCB  
843 and JFC have contributed to the final drafting of the article. LP have contributed to the design of the  
844 experiments and wrote the article. AKBS and HR have conceived, designed, acquired and analyzed  
845 data, and wrote the article.

846

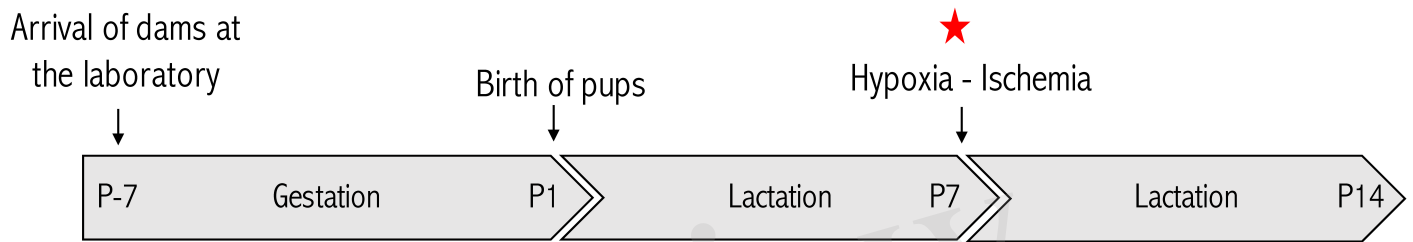
**847 9 Funding**

848 This work was supported by grants (2018/01) from the Fondation de Recherche en Alcoologie (FRA),  
849 from the French State in the context of the "Investments for the future" Programme IdEx (ANR-10-  
850 IDEX), the LabEx TRAIL(Translational Research and Advanced Imaging Laboratory) cluster of  
851 excellence of Bordeaux University (ANR-10-LABX-57) and the Department of Physiology, University  
852 of Lausanne. LP received financial support from the program IdEx Bordeaux ANR-10-IDEX-03-02.

853

In review

Figure 1.TIFF



sham	
shamrsv	→
HIC	★
rsvGL	→ ★
rsvL	→ ★
rsvG	→ ★
rsvC	→ ★ →

→ RSV in the drinking water for the dams

Figure 2.TIFF

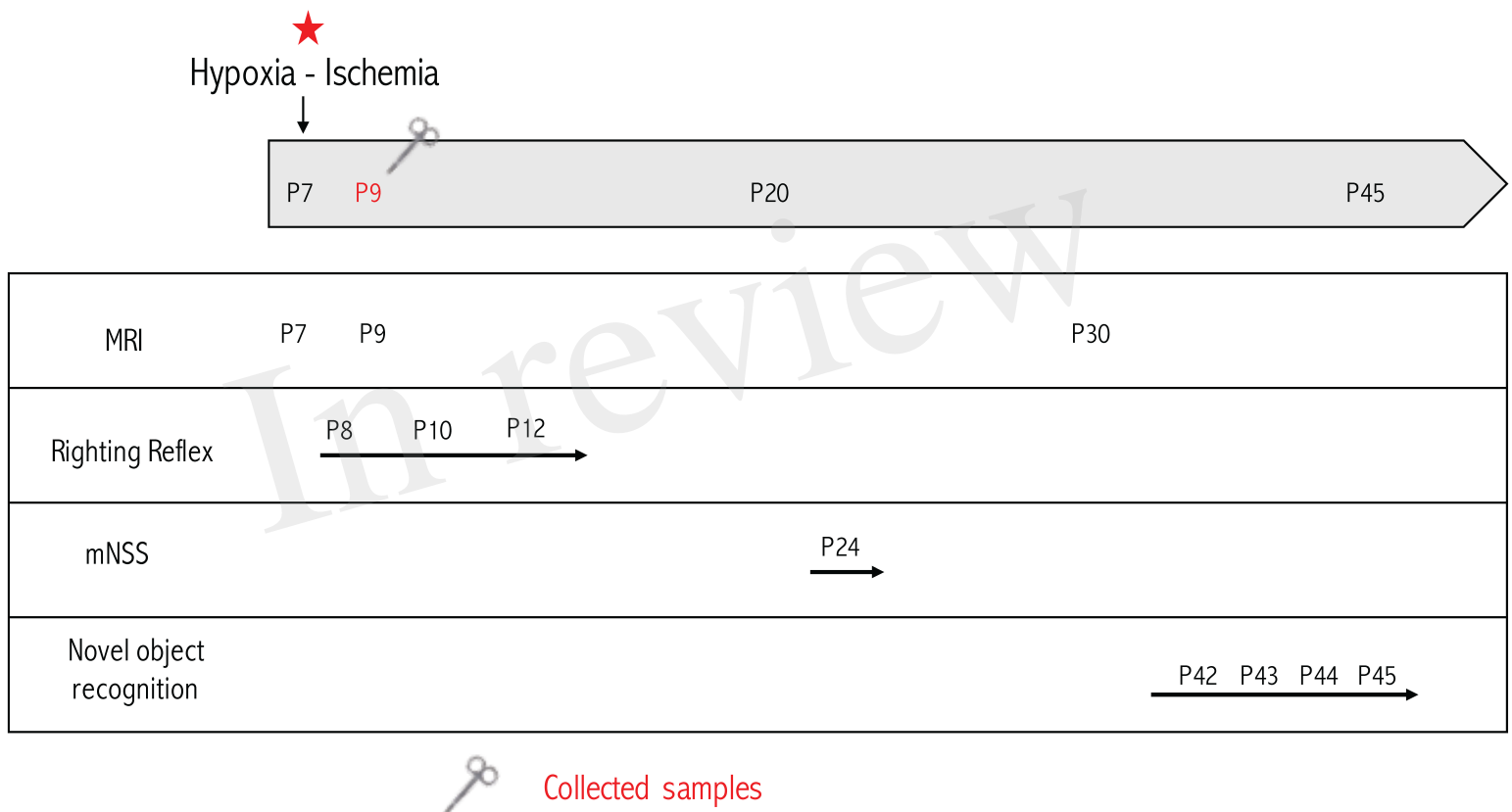


Figure 3.TIFF

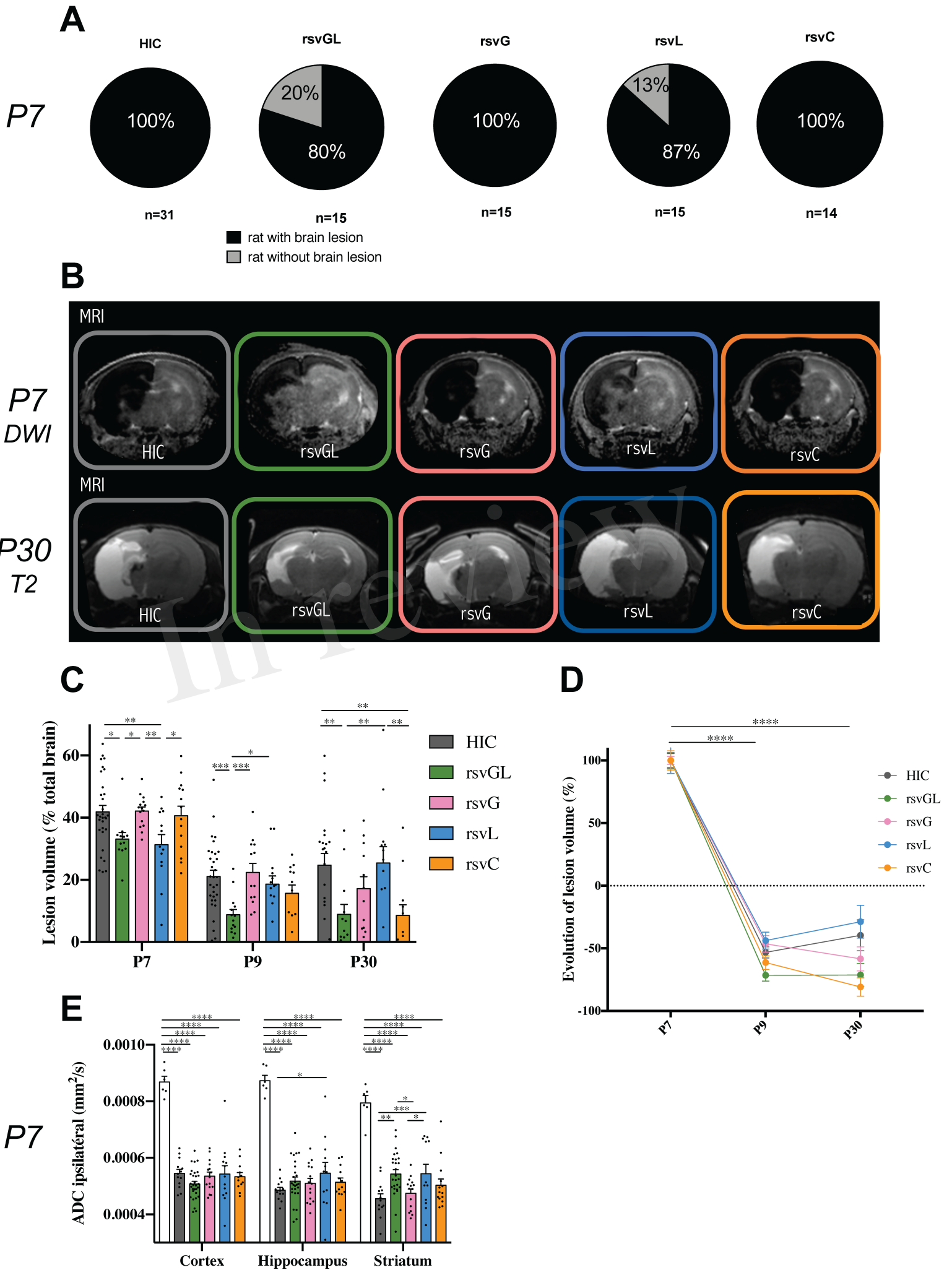


Figure 4.TIFF

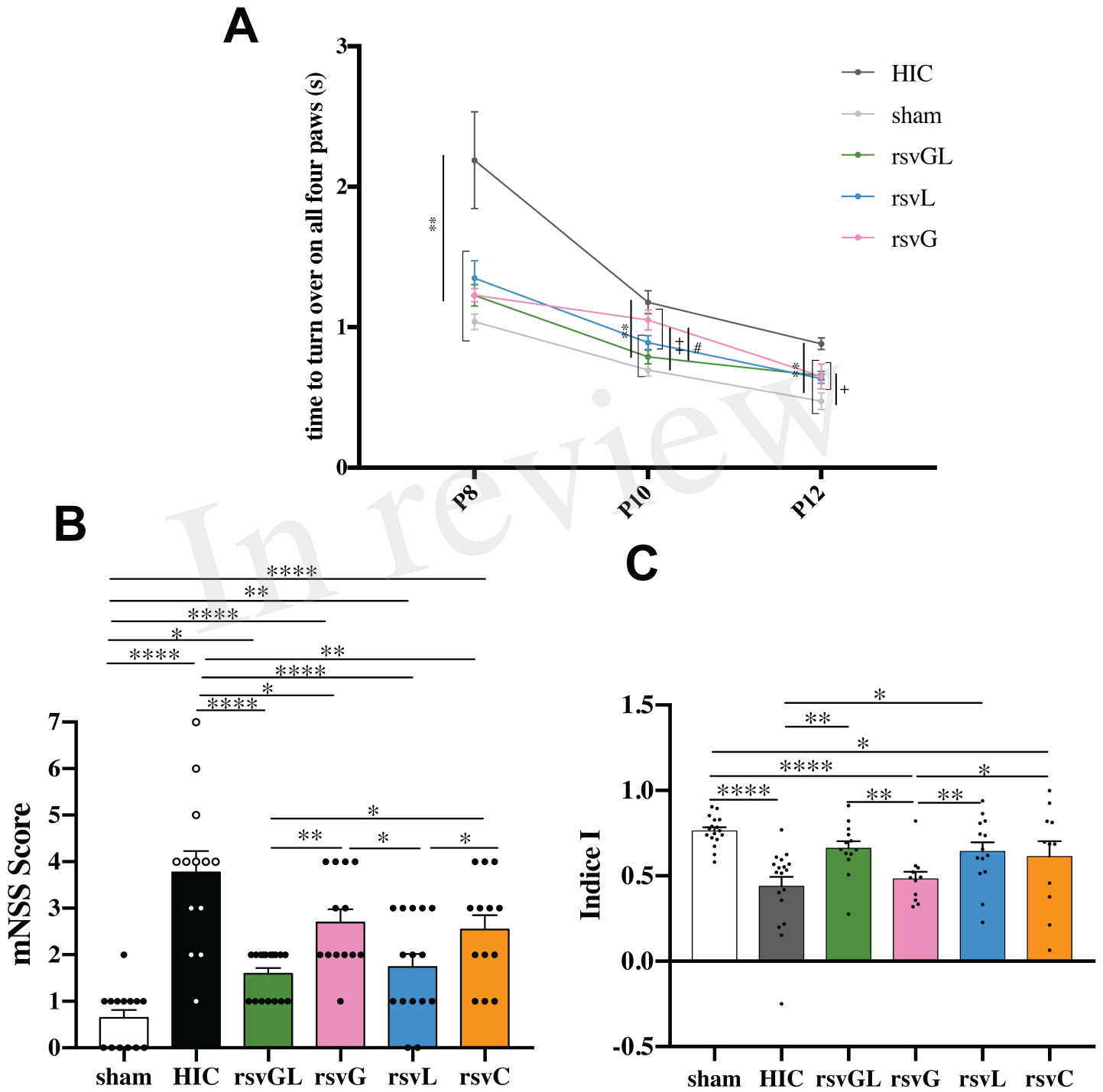
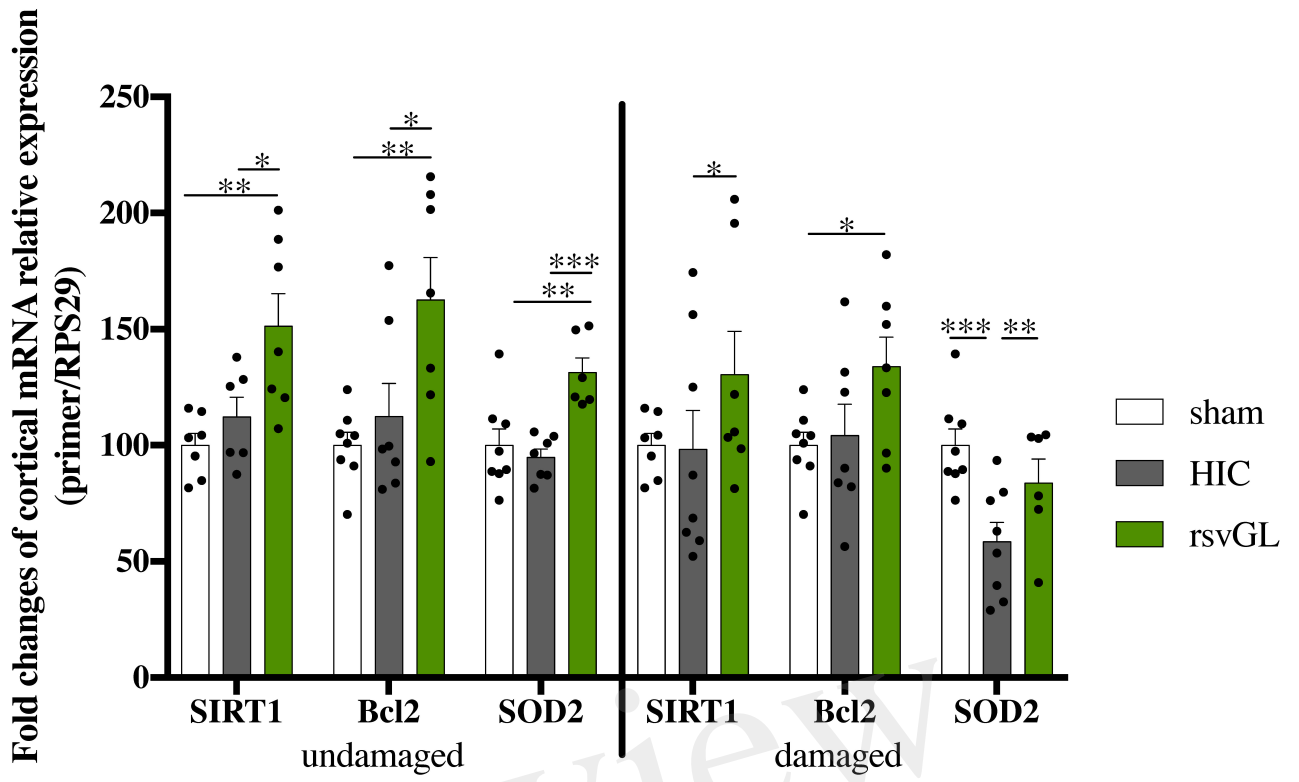


Figure 5.TIFF

**A**



**B**

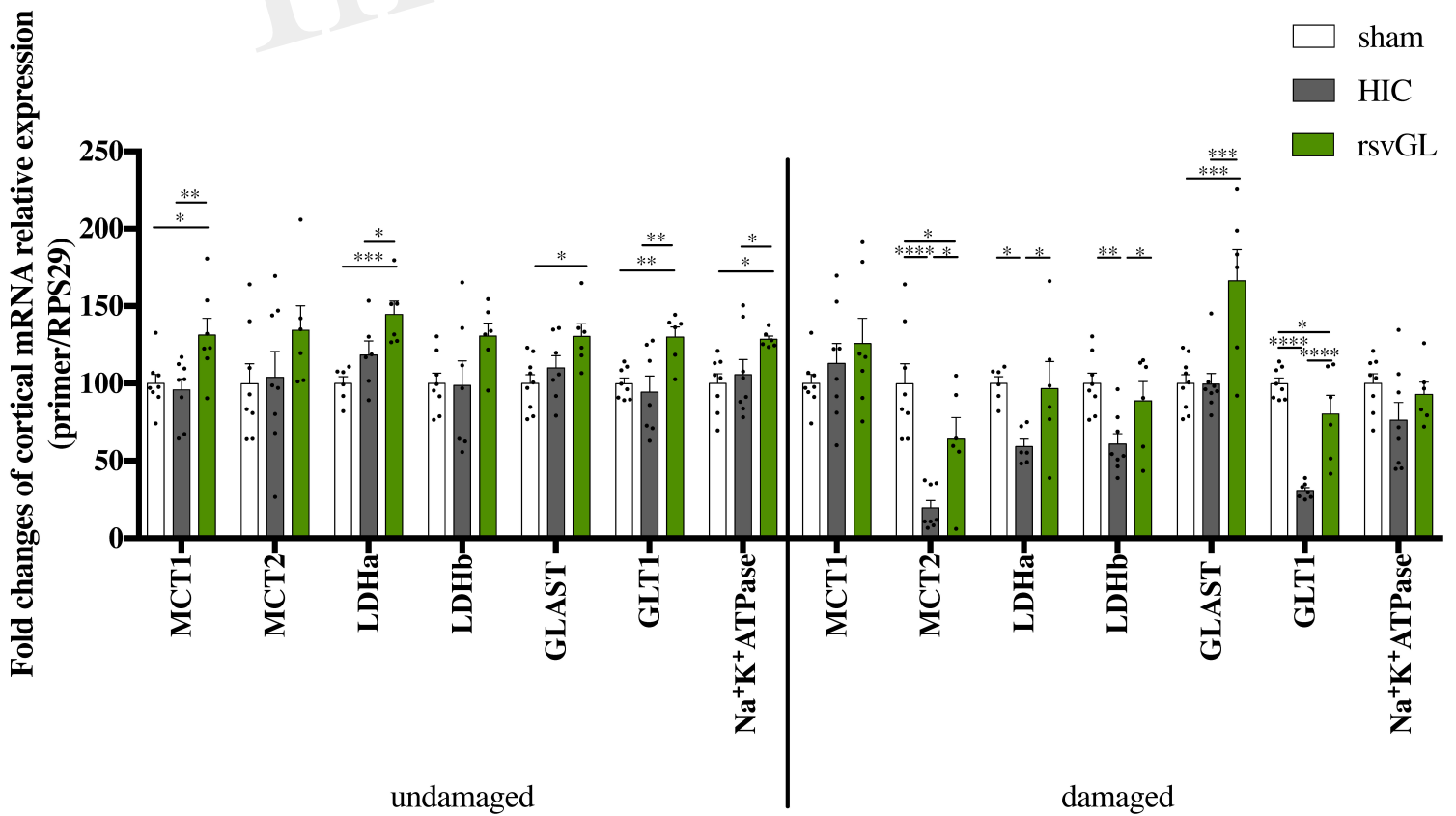


Figure 6.TIFF

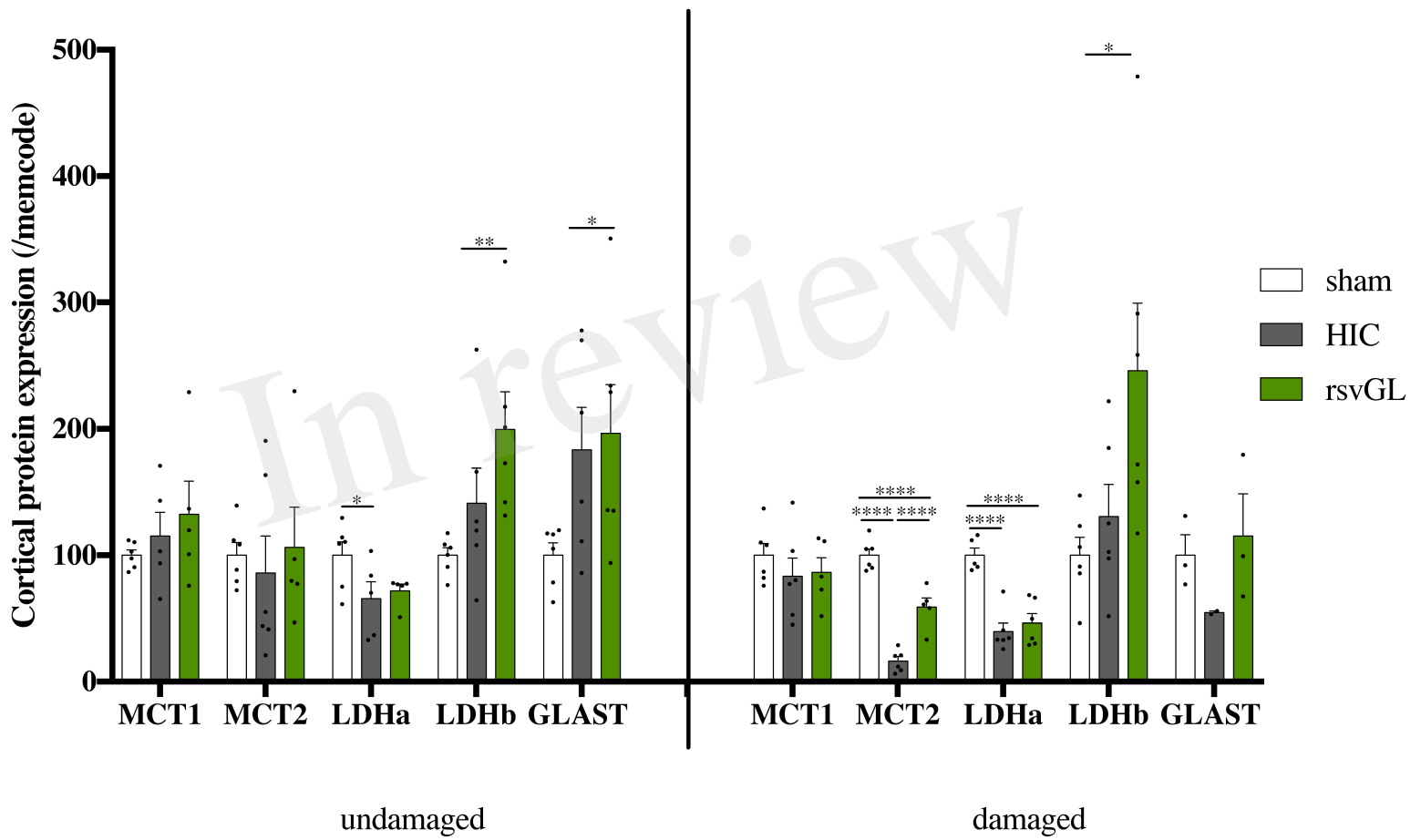


Figure 7.TIFF

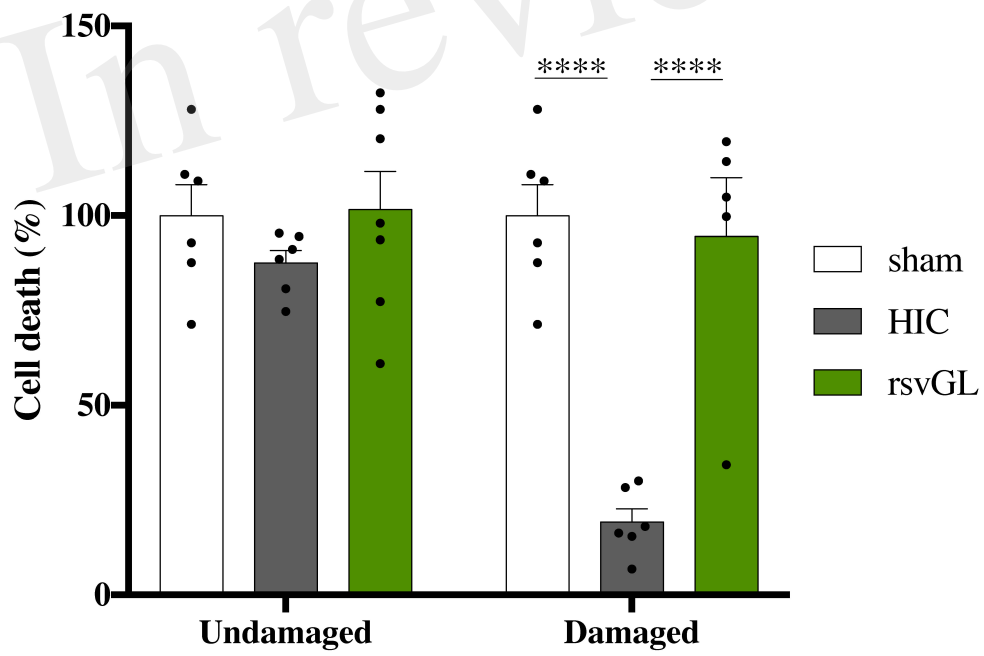
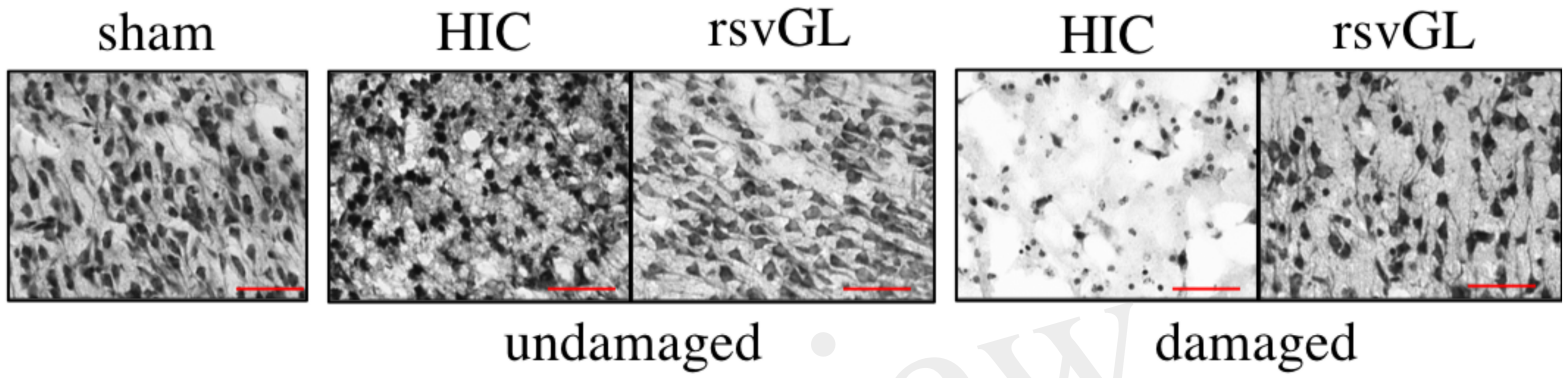


Figure 8.TIFF

